Changes of palaeoenvironmental conditions recorded in Late Devonian reef systems from the Canning Basin, Western Australia: A biomarker and stable isotope approach

Svenja Tulipani[a], Kliti Grice[a]*, Paul F. Greenwood[a,b], Peter W. Haines[c], Peter E. Sauer[d], Arndt Schimmelmann[d], Roger E. Summons[e], Clinton B. Foster[f,g], Michael E. Böttcher[h], Ted Playton[i], Lorenz Schwark[a,j]

[a] *Western Australian Organic and Isotope Geochemistry Centre, Department of Chemistry, Curtin University, The Institute for Geoscience Research, GPO Box U1987, Perth, WA 6845, Australia*

[b] *Centre for Exploration Targeting and Western Australian Biogeochemistry Centre, The University of Western Australia 35 Stirling Highway, Crawley, WA 6009, Australia*

[c] *Geological Survey of Western Australia, Department of Mines and Petroleum, 100 Plain Street, East Perth, WA 600, Australia*

[d] *Department of Geological Sciences, Indiana University, 1001 East 10th Street, Bloomington, IN 47405-1405, USA*

[e] *Department of Earth, Atmospheric and Planetary Sciences, MIT, E25-633, 45 Carleton Street Cambridge, MA 02139, USA*

[f] *Geoscience Australia, GPO Box 378 Canberra, ACT 2601, Australia*

[g] *School of Earth and Environment, The University of Western Australia 35 Stirling Highway, Crawley WA 6009, Australia*

[h] *Geochemistry & Isotope Geochemistry Group, Marine Geology Department, Leibniz-Institute for Baltic Sea Research, Seestrasse 15, D-18119 Warnemünde, Germany*

[i] *Chevron Energy Technology Company, Carbonate Stratigraphy Research & Development, 1500 Louisiana Street, Houston, TX 77002, USA*

[j] *Institute of Geoscience, Kiel University, Ludewig-Meyn Str. 10, 24118 Kiel, Germany*

*Corresponding authors: s.tulipani@curtin.edu.au, +61 (0)8 9266 7628;

k.grice@curtin.edu.au, +61 (0)8 9266 2474

Keywords:

Late Devonian, thermal maturity, MTTCs, C/N preservation, 4-methylsteranes

Abstract

Although the Late Devonian extinctions were amongst the largest mass extinction events in the Phanerozoic, causes, nature and timing of these events remain poorly restrained. In addition to the most pronounced biodiversity loss at the Frasnian-Famennian (F-F) boundary and the end Famennian, there were also less extensively studied extinction pulses in the Middle to Late Givetian and the Frasnian. Here we used a combination of palynological, elemental, molecular and stable isotope analyses to investigate a sedimentary record of reef-systems from this time period in the Canning Basin, Western Australia.

The acquired data generally showed distinct variations between sediments from (i) the time around the Givetian-Frasnian (G-F) boundary and (ii) later in the Frasnian and indicated a distinct interval of biotic stress, particularly for reef-builders, in the older sediments. Alterations of pristane/phytane ratios, gammacerane indices, *Chlorobi* biomarkers, $\delta D_{kerogen}$ and chroman ratios describe the change from a restricted marine palaeoenvironment with an anoxic/euxinic hypolimnion towards a presumably open marine setting with a vertically mixed oxic to suboxic water column. Simultaneous excursions in $\delta^{13}C$ profiles of carbonates, organic matter (OM) and hydrocarbons in the older sediments reflect the stratification-induced enhancement of OM-recycling by sulfate reducing bacteria. Alterations in sterane distributions and elevated abundances of methyltrimethyltridecylchromans (MTTCs) and perylene indicate an increased terrigenous nutrient input *via* riverine influx, which would have promoted stratification, phytoplankton blooms and the development of lower water column anoxia.

The detected palaeoenvironmental conditions around the G-F boundary may reflect a local or global extinction event. Our data furthermore suggest a contribution of the higher plant-expansion and photic zone euxinia to the Late Devonian extinctions, consistent with

previous hypotheses. Furthermore, this work might contribute to the understanding of variations in Devonian reef margin and platform-top architecture, relevant for petroleum exploration and development in the global Devonian hydrocarbon resources.

1. Introduction

In the Late Devonian some of the biggest mass extinctions in Earth's history ultimately wiped out the extensive reef systems prominent throughout that era (Sepkoski, 1986, 1993; Walliser, 1996; Bambach, 2006). The most pronounced extinction occurred at the Frasnian-Famennian (F-F) boundary; however there were also distinct biodiversity crises towards the end of the Givetian and Famennian as well as earlier in the Frasnian (Walliser, 1996; Caplan and Bustin, 1999; Aboussalam and Becker, 2001). Reef-building communities and associated fauna in tropical, shallow marine settings were the most severely affected organisms, whereas terrestrial ecosystems were only marginally impacted (Copper, 1986; Fagerstrom, 1994; McGhee, 1996). The cause(s) and nature (distinct events, several smaller pulses or gradual diversity decline) of the extinctions continue to be debated (e.g. McGhee, 1996; House, 2002; Racki, 2005). Hypotheses range from bolide impacts (McLaren, 1970, 1983; Ellwood et al., 2003; Sandberg et al., 2002) to climate change and rapid sea-level fluctuations in response to various parameters including atmospheric CO_2 reduction due to the rise of terrestrial plants or extensive volcanism (Murphy et al., 2000; Courtillot and Renne, 2003; McGhee, 2005; Algeo and Scheckler, 2010). The expanding terrestrial vegetation and the associated higher nutrient input from enhanced weathering and soil formation may have further contributed to the widespread anoxia and eutrophication in Late Devonian oceans, which have in particular (but not only) been linked to the F-F extinctions (Joachimski and Buggisch, 1993; Bond et al., 2004; Algeo and Scheckler, 2010). Whereas most research focuses on the investigation of the

F-F or end-Famennian extinctions, studies about earlier events in the Late-Givetian and Early- to Middle-Frasnian are comparatively rare.

Several Phanerozoic mass extinction events have been associated with oceanic anoxic events (OAEs) in which a stagnant water-column led to persistent stratification and widespread anoxia and photic zone euxinia (PZE; e.g. Grice et al., 2005b; Summons et al., 2006; Jenkyns, 2010; Nabbefeld et al., 2010d; Jaraula et al., 2013). The latter describes a condition where high concentrations of toxic hydrogen sulfide produced by anaerobic sulfate-reducing bacteria (SRB) in or near sediments expand into the photic zone (i.e. surface water layer with enough light penetration for photosynthesis). PZE may have also contributed to the Late Devonian extinctions since evidence of this condition has been reported in Middle- to Late Devonian sediments and crude oils from various locations including North America (Summons and Powell, 1986, 1987; Requejo et al., 1992; Brown and Kenig, 2004; Maslen et al., 2009), Europe (Marynowski et al., 2000, 2011; Joachimski et al., 2001; Marynowski and Filipiak, 2007) and Western Australia (Maslen et al., 2009; Melendez et al., 2013a, 2013b; Tulipani et al., 2014a).

Much of the ancient marine life of this time has been captured in the extensive and well-preserved Devonian reef systems of the Western Australian Canning Basin (e.g. Playford et al., 2009). The location is particularly well-known for the excellent preservation of macro- (Long and Trinajstic, 2010) and molecular fossils (i.e. biomarkers; Melendez et al., 2013a, 2013b) in sections of the Gogo Formation, the Middle Givetian to Middle Frasnian basin facies.

This manuscript presents data from comprehensive molecular, elemental (C, N, and S) and stable isotope analyses ($\delta^{13}C$ of biomarkers, organic matter (OM) and carbonates; $\delta^{18}O_{carbonates}$, $\delta D_{kerogen}$ and $\delta^{34}S_{pyrite}$) of sediments from a lower slope/basinal core from the Canning Basin, representing the time period from the earliest Frasnian (or potentially latest

Givetian) until later in the Frasnian. Our primary aim was to identify environmental conditions which may reveal causes and timeframes of potential extinction events whilst also extending our general interest in biomarker preservation in the Gogo Formation. A previous study (Tulipani et al., 2014a), which introduced a novel biomarker proxy for freshwater incursions in marine palaeoenvironments was based on the analysis of sediments from the lowermost section of this core. It revealed evidence of a persistently stratified water-column (freshwater lens overlying more saline hypolimnion), with prevailing anoxia and PZE in the corresponding depositional setting. Here we present a more comprehensive approach including additional parameters and a further extension of palaeoenvironmental reconstructions until later in the Frasnian.

2. Geological setting

The samples analysed here originate from a diamond drill core (MR-1) collected in 2010 at McWhae Ridge (18.72796°S, 126.0682°E), at the southern end of South Lawford Range along the Lennard Shelf, Canning Basin, Western Australia (Fig. 1a). The geological setting at this location is displayed in a cross section (Fig. 1b) and has been described elsewhere (e.g. Becker et al., 1991; Playford et al., 2009). In brief, it comprises a faulted reef spine (Pillara-Limestone, Givetian-Frasnian) which drowned in the Early Frasnian and was overlain by marginal slope (Sadler and Virgin Hills formations, Givetian-Middle Frasnian and Middle Frasnian-Famennian, respectively) and basin facies (Gogo Formation, Givetian-Middle Frasnian). In the latest Frasnian and Early Famennian it was overgrown by a now largely eroded deep-water microbial bioherm.

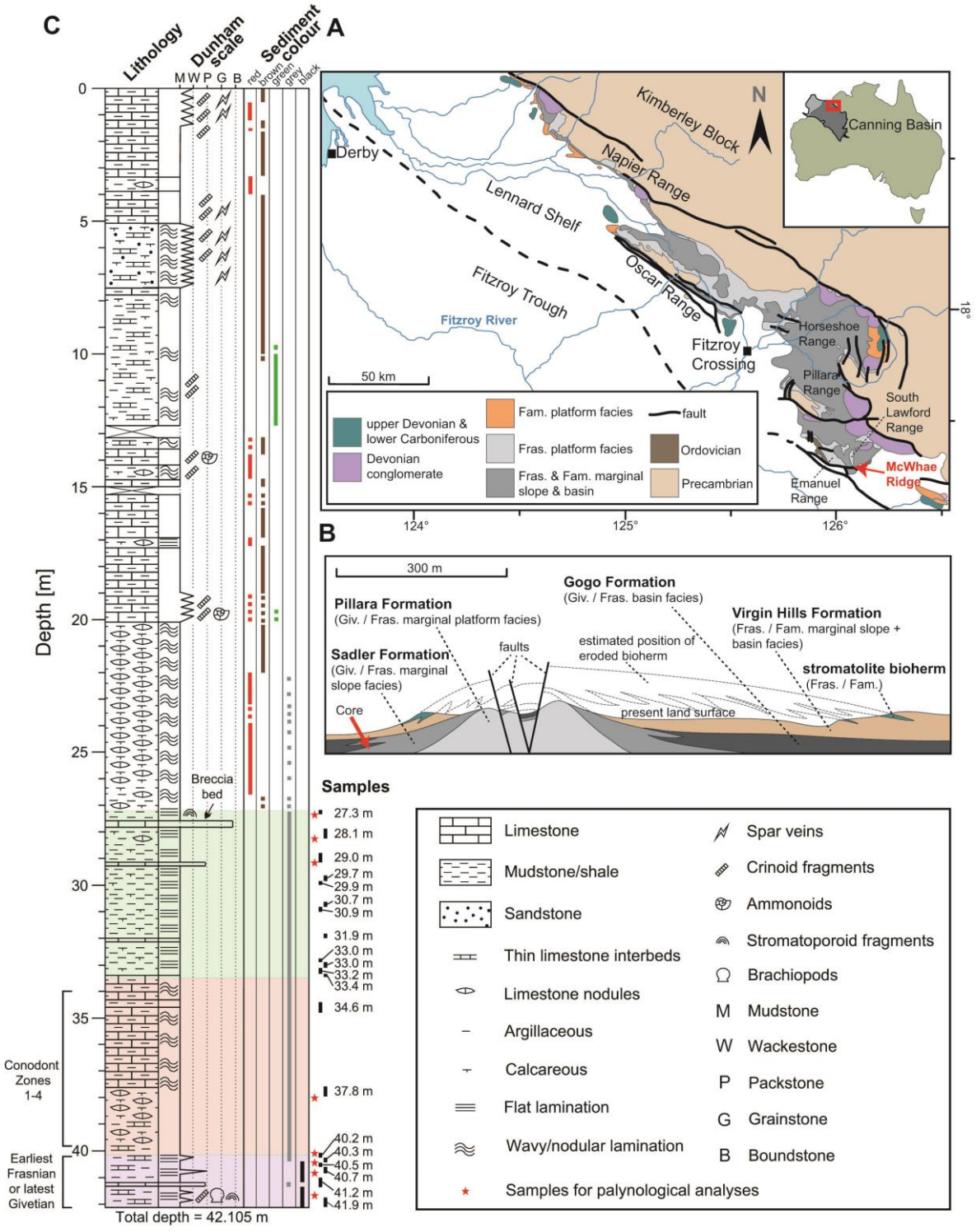

Figure 1: Location (A) and sedimentary log (B) of the core collected from McWhae Ridge. (C) Displays the geological setting at that location in a cross section. Background colours of the sedimentary log mark the lower, middle and upper intervals discussed in the text. Giv. = Givetian, Fras. = Frasnian, Fam. = Famennian. Samples are labelled with the medium depths. Map and cross section were modified after Playford et al. (2009). Conodont dates were obtained from personal communication Trinajstic and Roelofs. The lowest core section was assigned to the *Contagisporites optivus* var. *optivus-Cristatisporites triangularis* Zone of latest Givetian and earliest Frasnian age based on palynological evidence (see text section 2).

Fig. 1c shows the sedimentary log of the MR-1 core. The section sampled for the present study (27.2-42.1 m) consists of interfingering Sadler and Gogo formations. The lowest part of the sampled interval (40.1-42.1 m; hereafter referred to as "lower interval") comprises the Gogo Formation and is of latest Givetian-earliest Frasnian age based on palynological analysis. The recovered plant microfossil assemblages include key species: *Geminospora lemurata* Balme 1962, *Medusapora dringii* Balme 1988, *Emphanisporites rotatus* McGregor 1961 (single specimen), *Verrucosisporites premnus* Richardson 1965, *Retusotriletes sp*. cf. *R. pychovii Naumova* 1953, and *Archaeozonotriletes timanicus* Naumova 1953. The latter has previously been recorded in Canning Basin assemblages from the Gogo Formation/Sadler Limestone/Pillar Limestone by Grey (1992); and McGregor and Playford (1992) list this taxon as a characteristic element of Australian plant microfossil assemblages assigned to the *Contagisporites optivus* var. *optivus*-*Cristatisporites triangularis* Zone of late Givetian and early Frasnian age. Other palynomorphs, predominant phytoplankton, indicate a saline/marine environment of deposition: spinose acritarchs, including *Solarisphaeridium spinoglobosum* (Staplin) Wicander 1974, *Solarisphaeridium spp.* and *Veryhachium sp. cf. V. colemanii* Playford 1981; thick-walled large, smooth leiospheres (Leioshaeridia spp.); scolecodont fragments (polychaete dentary remains) and acritarchs assigned to *Dictyotidium sp.* and *Lomatolopas cellulosa* Playford 1981. The interval consists of black laminated argillaceous shales with thin limestone interbeds and some narrow irregular beds of shelly wackestone and fine grained packstone. Brachiopods, crinoids and stromatoporoid fragments are abundant (see Fig. 1c). The section is followed by an OM-lean interval (33.5-40.1 m; hereafter referred to as "middle interval") of irregular bedded grey or pale yellowish-grey calcareous siltstone with abundant micrite nodules (37.5-40.1 m) and argillaceous limestone (33.5-37.5 m). The uppermost part of the sampled interval (27.2-33.5 m; hereafter referred to as "upper interval") consists of medium grey finely

laminated calcareous shale and a few thin beds of nodular and brecciated micrite and fine packstone. Towards the top of this interval the calcareous content increases whereas lamination decreases. The interval between 34.0 and 39.8 m corresponds to conodont zones 1-4 (personal communication Trinajstic and Roelofs) of an international Upper Devonian zonation scheme (Klapper, 2007). In the remaining core sections conodont dating could not be performed due to a lack of specimen.

The uppermost core-section (above 27.2 m), which has not been considered here due the low OM-content, includes the F-F boundary between 3-5 m and consists of the Virgin Hills Formation.

From the Late Givetian to the Middle Frasnian, a long-term global rise in relative sea-level led to the retreat and backstepping of reefal margins in the Canning Basin. Subsequently, a decrease in tectonic subsidence rates coupled with global eustatic sea-level fall in the Late Frasnian and Famennian resulted in prograding platform margins (Playford et al., 2009).

3. Experimental

Analytical methods and sample preparation are described in the supplementary material (SM).

4. Results and discussion

The three different intervals of the sampled core section described in "2. Geological setting" (lower interval deposited close to or at the G-F boundary, 40.1-42.1 m; middle and upper interval deposited in the Frasnian, 33.5-40.1 m and 27.2-33.5 m, respectively; see Fig. 1) each show strong differences in the analytical data, reflecting distinct palaeoenvironments. Due to the low OM-content the middle interval is represented by one sample only.

4.1 Aliphatic hydrocarbons

Fig. 2 displays a typical total ion chromatogram (TIC) from gas chromatography-mass spectrometry (GC-MS) analyses of aliphatic fractions in sediments from the lower interval deposited around the G-F boundary (Fig. 2a) and the upper interval deposited later in the Frasnian (Fig. 2b). All aliphatic fractions (except the one from the OM-lean middle interval), contained abundant *n*-alkanes with chain lengths from C_{13}, C_{14}, or (occasionally) C_{15} to C_{33}. Their distributions typically maximised at C_{21} and showed a slight odd-over-even predominance in shorter as well as longer chain lengths (see carbon preference indices, CPIs, in Table 1). *n*-Alkanes in sediments from the middle interval were present at low concentrations and ranged from C_{16} to C_{33}. The isoprenoids pristane (**I**, Fig. S1) and phytane (**II**) were present in all samples and dominated the aliphatic fractions of sediments from the lower interval. Furthermore, all samples revealed complex distributions of saturated and unsaturated hopanoids and steroids. The most abundant of these were C_{27} to C_{29} diaster-(13)17-enes (**III**) highlighted in the *m/z* 257 mass chromatograms in Fig. 2. The hopanoids included C_{29} to C_{35} regular hopanes with 17β,21β (ββ), 17β,21α (βα) and 17α,21β (αβ) configurations (**IV**) as well as 18α 22,29,30-trisnorhopane (Ts), 17α 22,29,30-trisnorhopane (Tm) and 17β 22,29,30-trisnorhopane (Tm-β; Fig. S2). 28,30-dinorhopane (DNH; Fig. S2) and C_{31} to C_{36} 2β and 3β methylhopanes were detected in relatively low concentrations (Fig. S3). Hopenes included hop-(13)18-enes and C_{30} to C_{35} hop-(17)21-enes (Fig. S4). Regular steranes were present in the 5α,14α,17α (ααα), 5α,14β,17β (αββ) and 5β,14α,17α (βαα) configurations (**V**) from C_{27} to C_{30} (Fig. S5). 3 and 4 methyl 24-ethylcholestanes and gammacerane (**VI**) were only present in significant concentrations in the lower interval. The same applied for C_{30} 3- or 4-methyl diasterenes (*m/z* 271 mass chromatogram, not displayed here).

Table 1: Selected elemental and molecular maturity parameters throughout the MR-1 core indicating an exceptionally low thermal maturity. T_{max} was determined by Rock Eval analysis. Ts = 18α 22,29,30-trisnorhopane; Tm = 17α 22,29,30-trisnorhopane. $C_{31}H$ = 17α,21β homohopane; C_{29} ααα St = 5α,14α,17α 24-ethylcholestane; S and R represent the stereochemistry at C22 and C20 for hopanes and steranes, respectively. CPI stands for carbon preference index and was calculated according to $\sum C_{odd}/\sum C_{even}$ over the range of C_{16} to C_{22} and C_{23}-C_{33}, respectively.

Depth [m]	T_{max} [°C]	Ts/(Ts+Tm)	$C_{31}H$ S/(S+R)	C_{29} ααα St S/(S+R)	CPI (C_{15}-C_{22})	CPI (C_{23}-C_{33})
27.3	*413	0.14	0.18	0.14	1.07	1.53
28.1	*410	0.15	0.16	0.15	1.18	1.59
29.0	*418	0.13	0.15	0.12	1.16	1.49
29.7	*409	n.d.	n.d.	n.d.	n.d.	n.d.
29.9	*407	0.14	0.15	0.04	1.18	1.58
30.7	*405	0.14	0.14	0.12	1.12	1.53
30.9	*421	0.14	0.15	0.11	1.20	1.82
31.9	*405	0.16	0.14	0.11	1.11	1.16
32.8	*406	0.18	0.16	0.10	1.02	1.46
33.0	*410	0.18	0.16	0.11	1.10	1.47
33.2	*415	0.19	0.16	0.10	0.93	1.18
33.4	*410	0.18	0.20	0.08	0.97	1.00
34.6	*417	n.d.	n.d.	n.d.	n.d.	n.d.
37.8	n.d.	0.47	0.36	0.19	1.04	1.03
40.2	n.d.	0.22	*0.23	0.08	1.43	1.30
40.3	*415	0.16	*0.20	0.09	1.27	1.20
40.5	*413	n.d.	n.d.	n.d.	1.00	0.89
40.7	*414	0.13	*0.13	0.09	1.04	1.13
41.2	*410	0.10	*0.12	0.09	1.07	1.24
41.9	*413	0.11	*0.11	0.09	1.00	1.16

* published in (Tulipani et al., 2014a)

4.2 Aromatic hydrocarbons

All aromatic fractions were dominated by the 5,7,8-trimethyl-2-methyltrimethyltridecylchroman (**VII**; triMeMTTC). Other common geological MTTCs (Fig. S1; Sinninghe Damsté et al., 1987) were also present but exhibited lower concentrations. Sediments from the lower interval furthermore contained a series of abundant mono- and diaryl isoprenoids (**VIII**) including intact iso (**IX**)- and palaeorenieratane (**X**; Figs. 3 and 4). Polyaromatic hydrocarbons (PAHs) were present at low abundances and included typical combustion markers such as benzo[*a*]pyrene (**XI**), benzo[*e*]pyrene (**XII**), coronene (**XIII**), benzo[*ghi*]perylene (**XIV**), fluoranthenes (**XV**) or pyrenes (**XVI**) as well as the presumably fungal-derived perylene (**XVII**; e.g. Grice et al., 2009).

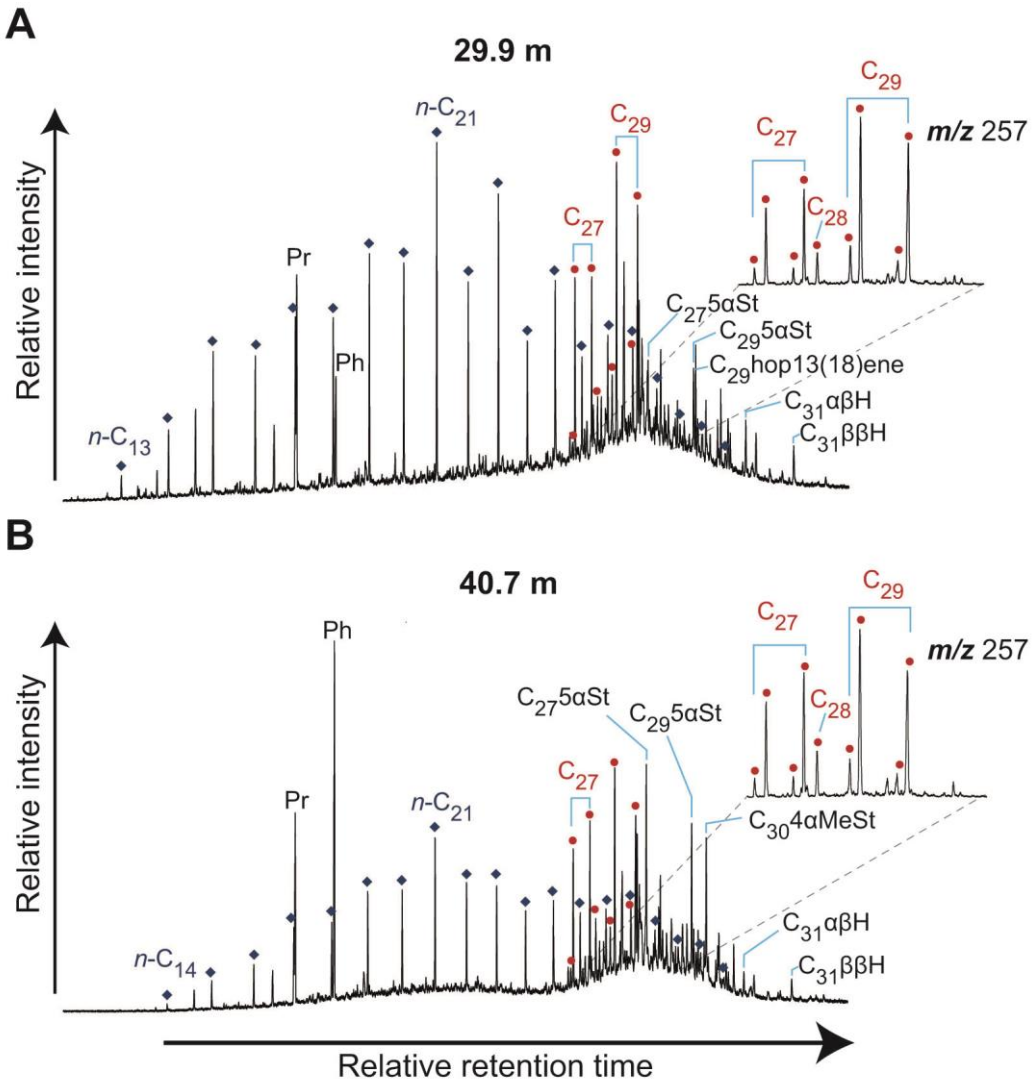

Figure 2: Total ion chromatograms showing two representative aliphatic fractions of samples deposited in (A) the earliest Frasnian or latest Givetian under anoxic/euxinic conditions, referred to as lower interval in the text (40.7 m) and (B) later in the Frasnian in a more oxic setting referred to as upper interval in the text (29.9 m), respectively. Extracted ion chromatograms of *m/z* 257 show distributions of C_{27}–C_{29} diaster-13(17)-enes with carbon number C_i. Not all isomers of the C_{28} diaster-13(17)-enes could be identified due to coelutions with more abundant C_{27} and C_{29} isomers. Red dots represent diasterenes, blue diamonds *n*-alkanes. 5αSt = regular 5α,14α,17α 20R steranes; C_{30}4αMeSt = 4α methyl-5α,14α,17α 20R 24-ethylcholestane; C_{31}αβH and C_{31}ββH = 17α,21β and 17β,21β 22R homohopane.

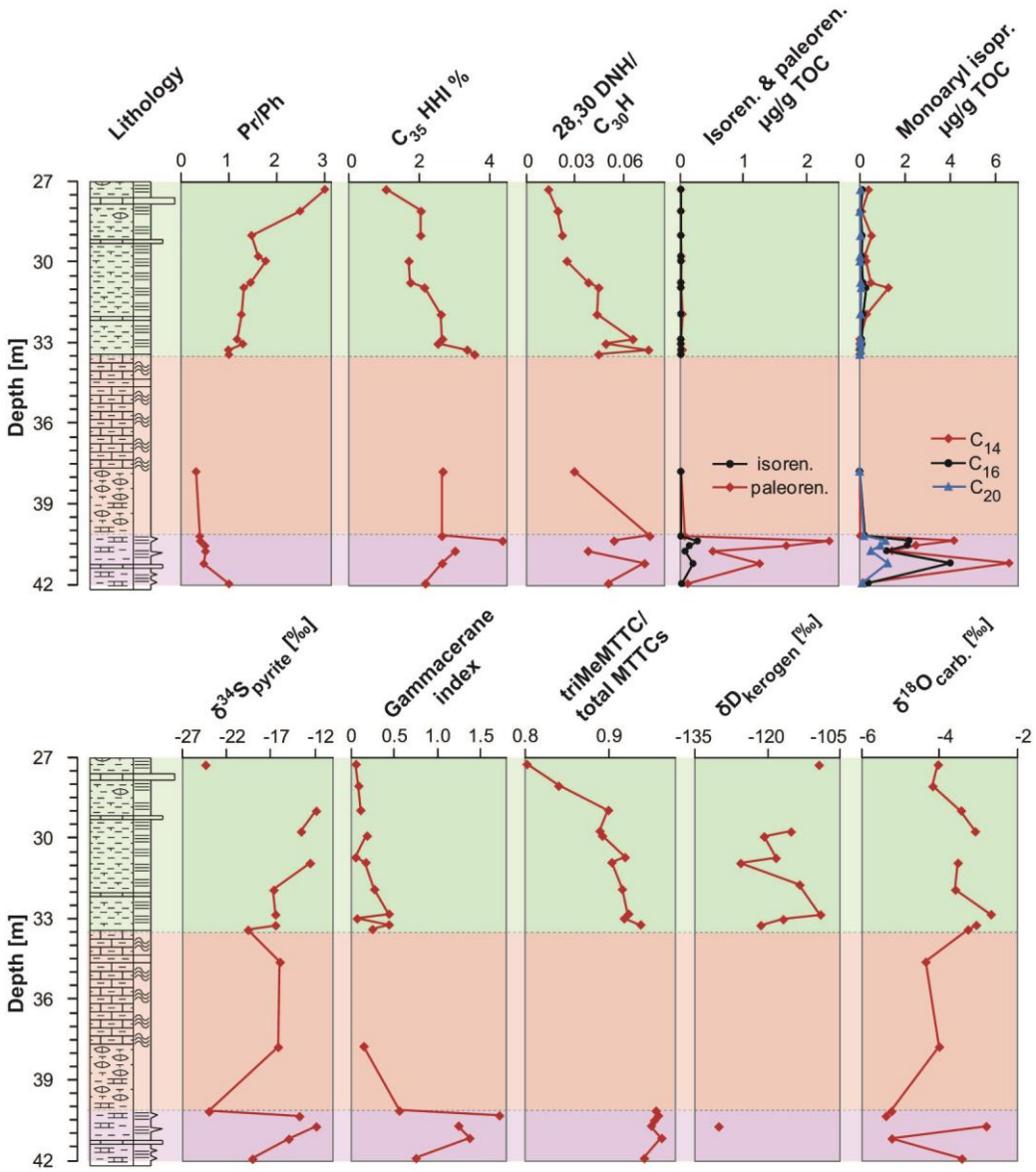

Figure 3: Depth profiles of stable isotope and biomarker parameters (potentially) indicative of redox conditions, photic zone euxinia, water-column stratification and salinity throughout the MR-1 core. Background colours mark the lower, middle and upper intervals discussed in the text. Pr/Ph = pristane/phytane; C_{35}HHI % stands for C_{35} homohopane index and was calculated according to: C_{35} homohopanes/$\sum$(C_{31} – C_{35} homohopanes)×100 %; 28,30 DNH/C_{30}H = 28,30 dinorhopane/17α,21β hopane; gammacerane index = gammacerane/17α,21β hopane; the three previous parameters were calculated from peak areas in suitable MRM-GC-MS transitions. Isoren. = isorenieatane; palaeoren. = palaeorenieratane; isopr. = isoprenoids; triMeMTTC/total MTTC = 5,7,8 trimethyl-2-methyltrimethyltridecylchroman/total methyltrimethyltridecylchromans, calculated from peak areas of selected ion monitoring traces; carb. = carbonates. δ^{34}S was reported in ‰ relative to VCDT; δD was reported in ‰ relative to VSMOW and has been corrected for exchangeable hydrogen according to Schimmelmann (1991); δ^{18}O was reported in ‰ relative to VPDB. Where gaps in the profiles are shown, the analyses have only been performed on selected samples or the determination was not possible. Some of the included data have already been presented in a different context in Tulipani et al. (2014a), see Table S1.

4.3 Evidence of water-column stratification, anoxia and PZE

The Late Givetian-Early Frasnian palaeoenvironmental setting corresponding to the lower interval has been described previously in Tulipani et al. (2014a). To summarize, enhanced gammacerane indices indicated a stratified water-column which promoted the development of PZE, evident in the abundance of palaeorenieratane (**II**) and other *Chlorobi* carotenoid derivatives. Low pristane/phytane ratios (Pr/Ph < 1) indicated anoxia and higher salinities in the hypolimnion and sediments whereas high chroman ratios (triMeMTTC/total MTTCs > 0.9) reflected the low salinities in an overlying freshwater lens from most likely predominantly riverine incursions. High abundances of perylene and MTTCs presumably represented significant terrigenous input.

Fig. 3 shows sediment depth profiles of the measured molecular and stable isotope indicators of redox conditions, salinity, stratification and PZE, which will be discussed in the following sections.

4.3.1 Indicators of palaeoenvironmental anoxia

The Pr/Ph ratio, the C_{35} homohopane index (C_{35} homohopanes/ $\sum(C_{31}$-C_{35} homohopanes)) and the relative abundance of 28,30-DNH displayed in Fig. 3 are commonly used redox indicators. Pr/Ph ratios in the upper interval were all > 1 and significantly higher than in the lower interval. In the two uppermost samples Pr/Ph showed a further increase. Also the C_{35} homohopane index and the relative abundance of 28,30-DNH showed distinct trends between these intervals with higher values in the lower core section.

Although Pr/Ph is one of the most frequently used molecular redox indicators, it can also be influenced by other palaeoenvironmental conditions, particularly salinity (ten Haven et al., 1985; Schwark et al., 1998). The higher Pr/Ph ratios in the upper interval indicate less reducing conditions and lower salinities in the hypolimnion/sediments in the depositional

environment (Fig. 3). In the two uppermost samples the further Pr/Ph increase to values approaching 3, reflects a well-mixed, oxygenated palaeo water-column.

The C_{35} homohopane index and the relative 28,30-DNH abundance are also influenced by additional factors such as type of source organism (e.g. Obermajer et al., 2000), composition of the sediment (e.g. clay contents) or thermal maturity (e.g. Peters and Moldowan, 1991; Peters et al., 2005). Nevertheless, the general trend of more oxygenated conditions in the upper interval evident in the Pr/Ph profile is also supported by the lower values of C_{35} homohopane index and relative 28,30-DNH abundance in this core section (e.g. Peters and Moldowan, 1991; Peters et al., 2005, and references therein). However, increased values for the C_{35} homohopane index and relative 28,30 DNH abundance in samples around 33 m depth indicate anoxic condition whereas Pr/Ph ratios were > 1, indicative of more oxic conditions.

Generally, the observed increase of water-column oxygenation in sediments from the upper interval is consistent with a more open setting at higher sea-levels later in the Frasnian (Playford et al., 2009).

4.3.2 Chlorobi carotenoid derivatives

Chlorobi (green sulfur bacteria) are obligately anaerobic, phototrophs which use hydrogen sulfide as an electron donor and therefore only thrive in the water-column under photic zone euxinic conditions. Palaeoenvironmental PZE is thus often characterized by the sedimentary abundance of their carotenoid derivatives. In the core analysed here the intact C_{40}-carotenoid pigments isorenieratane, palaeorenieratane and renieratane (**XVIII**), were only abundant in sediments from the lower interval. In contrast, monoaryl isoprenoids were also present at low concentrations in the remaining samples (Fig. 3). Whilst the intact carotenoids are exclusively derived from *Chlorobi* and hence unambiguously indicate PZE (e.g.

Summons and Powell, 1986; Schwark and Frimmel, 2004; Grice et al., 2005b), monoaryl isoprenoids may have additional sources (e.g. Grice et al., 1996; Koopmans et al., 1996). This is also confirmed by the average $\delta^{13}C$ values of aryl isoprenoids in samples from the lower interval (Fig.4). The ^{13}C-enriched signatures are typical of lipids synthesised *via* the reductive tricarboxylic acid (TCA) cycle used by *Chlorobi* (Quandt et al., 1977; Sirevåg et al., 1977). The more negative $\delta^{13}C$ values of most lower-molecular-weight aryl isoprenoids compared to palaeorenieratane, may reflect additional sources other than *Chlorobi*.

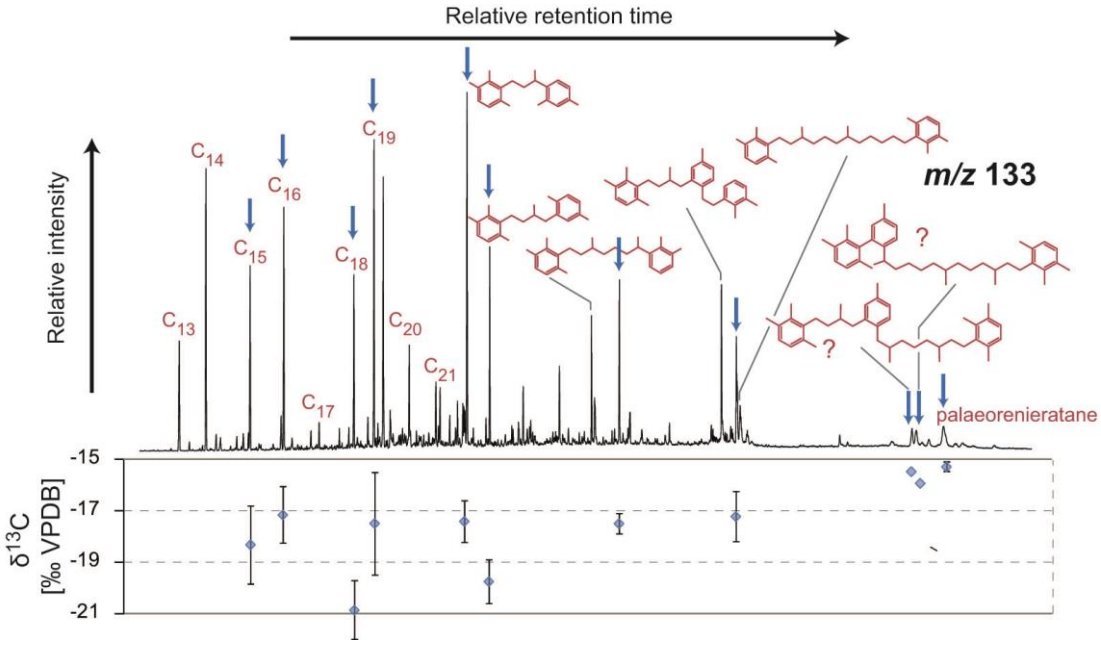

Figure 4: *Chlorobi* carotenoid derivatives in the *m/z* 133 trace from selected ion monitoring (SIM) GC-MS of a representative sample in the lower interval of the analysed core corresponding to the Late Givetian-Early Frasnian (depth 40.7 m). "C_i" mark monoaryl isoprenoids with carbon number "i". $\delta^{13}C$ values represent the average for the respective compound in all samples below 40.1 m with error bars indicating the standard deviations. The two values without error bars could only be measured in 1 sample. Blue arrows indicate the peak corresponding to the respective $\delta^{13}C$ value. Question-marks indicate tentatively identified structures. The chromatogram as well as the stable isotopic composition of palaeorenieratane have been published in Tulipani et al. (2014a).

4.3.3 $\delta^{34}S$ of pyrite

$\delta^{34}S$ signatures of total reduced inorganic sulfur (~pyrite) throughout the core ranged from -24.4 to -11.9 ‰ (Fig. 3). Similar $\delta^{34}S$ values were previously reported in some

European Late Devonian sediments (Joachimski et al., 2001) although sediments from Northern America, Southern China and Poland from the same time period showed more positive values (Goodfellow and Jonasson, 1984; Chen et al., 2013). The current data are similar to $\delta^{34}S$ values measured in sediments of the modern euxinic Baltic Sea (Böttcher and Lepland, 2000; Böttcher et al., 2012) and of eastern Mediterranean hypersaline basins (Ziebis et al., 2000) but less ^{34}S-depleted when compared to the modern Black Sea (Fry et al., 1991; Jørgensen et al., 2004; Neretin et al., 2004).

The strong ^{34}S-depletion compared to the estimated value of Devonian sea-water (+15 and +20 ‰; Kampschulte and Strauss, 2004; Wortmann and Paytan, 2012) indicates that microbial sulfate reduction occurred in surface sediments or the water-column where it was not significantly limited by the abundance of dissolved sulfate (essentially 'open system' conditions; (e.g. Canfield and Teske, 1996; Hartmann and Nielsen, 2012) independent from any salinity changes. Estimated overall sulfur isotope fractionation factors range between -27 and -44 ‰, which is in the range observed at low to moderate cellular sulfate reduction rates in SRB cultured on simple organic substrates (Kaplan and Rittenberg, 1964; Chambers and Trudinger, 1979; Sim et al., 2011).

4.3.4 Gammacerane index

Gammacerane indices in the upper interval were significantly lower than in sediments from the lower interval (Fig. 3). This suggests a vertically mixed water-column later in the Frasnian, contrary to the conditions around the G-F boundary. Gammacerane is sourced from tetrahymanol in bacterivorous ciliates living exclusively at the chemocline and therefore is an indicator for water-column stratification (Harvey and McManus, 1991; Sinninghe Damsté et al., 1995; Grice et al., 1998; Tulipani et al., 2014a). A well-mixed water column in palaeoenvironments from the upper interval (in particular the uppermost two samples) is also

consistent with the lower chroman ratios in that core section (Fig. 3) reflecting higher salinities in the epilimnion (Tulipani et al., 2014a).

4.3.5 δD of kerogen

The δD values of kerogens were more positive in sediments from the upper interval compared to those from the lower interval (Fig.3). However, due to the technical challenges of δD analysis and time consuming sample preparation, only one sample from the lower interval was analysed and therefore this value might not be entirely representative. For the determination of δD values only non-exchangeable hydrogen, which does not interact with aqueous hydrogen during diagenesis, was included (Schimmelmann et al. 1999; 2006. Nevertheless it potentially could be replaced during later stages of thermal maturation (e.g. Dawson et al., 2005, 2007; Pedentchouk et al., 2006; Schimmelmann et al., 2006; Maslen et al., 2013). However, due to the very low thermal maturity of the analysed kerogens (section 4.4), the measured δD values are likely representative of the palaeoenvironment (Hassan and Spalding, 2001; Lis et al., 2006; Nabbefeld et al., 2010a).

Generally, δD signatures of biomass are strongly influenced by the D/H composition of the source water used for biosynthesis (Sessions et al., 1999; Dawson et al., 2004; Grice et al., 2008; Nabbefeld et al., 2010a; Zhou et al., 2011). Therefore the comparatively D-depleted value representing the lower interval potentially reflects the freshwater incursions (evident in elevated chroman ratios (Tulipani et al., 2014a)), which typically lead to a D-depletion in the marine environment. Due to fractionation effects in the hydrological cycle, meteoric waters are generally more D-depleted than seawater, which exhibits a δD value of ~0 (Gat, 1996). Furthermore, the variations in the δD profile could represent changes in the type of source organisms or growth forms (Nabbefeld et al., 2010c; Polissar and Freeman, 2010). It is likely

that the lower δD value of the lowermost sample may have additionally been influenced by greater input from D-depleted terrestrial biomass of organisms utilizing meteoric waters.

4.3.6 $\delta^{18}O$ of carbonates

$\delta^{18}O$ values of carbonates in the lower interval corresponding to the anoxic/euxinic palaeoenvironment with freshwater incursions showed significant variations, but were on average more ^{18}O-depleted than carbonates in the remaining core sections (Fig. 3). $\delta^{18}O$ and $\delta^{13}C$ values of carbonates showed only a slight correlation ($R^2 = 0.3$; Fig. S6) indicating separate influences on both parameters and most likely no significant diagenetic control. Typically, $\delta^{18}O$ signatures of carbonates are representative of the stable isotopic composition of the corresponding source water (e.g. Sachse et al., 2004). Therefore the greater ^{18}O-depletion of some samples from the lower interval might be indicative of freshwater incursions since meteoric and run-off waters are depleted in heavy isotopes.

4.4 Thermal maturity and OM-preservation

For their Palaeozoic age the analysed sediments showed an exceptionally low thermal maturity, evident in elemental as well as molecular maturity parameters (Table 1). This was also confirmed by pale to mid to yellow spore colours (Thermal Alteration Index (TAI; Staplin, 1969)). T_{max} values from Rock Eval analysis were all < 421 °C (average: 411.7 °C; Table 1) reflecting a very low thermal alteration (e.g. Peters et al., 2005). Furthermore, high abundances of hopane and sterane isomers in their biological configuration relative to the more thermally stable geological isomers were evident in very low ratios of homohopane isomerisation at C22, ααα 24-ethylcholestane isomerisation at C20 and Ts *vs.* Tm (Table 1). All of these values, with the exception of the OM- lean sample at 37.8 m, correspond to

vitrinite reflectance equivalents < 0.5 % and mostly < 0.4 % (Hulen and Collister, 1999), indicating burial heating < 80 and < 60 °C, respectively (Barker and Pawlewicz, 1994).

The high abundances of unsaturated hopanoids and steroids were also highly unusual for Palaeozoic sediments as the double-bonds are usually cleaved during relatively early stages of diagenesis (e.g. Mackenzie et al., 1982; Peters et al., 2005). Regular steranes were generally much more abundant than their corresponding diasteranes (Fig. S4), which is typical of relatively immature carbonate-rich and clay-poor sediments (e.g. Nabbefeld et al., 2010b). However, diasterenes, which represent diagenetic precursors of diasteranes (Mackenzie et al., 1982) were quite prominent (Fig. 2).

A low thermal maturity based on molecular ratios has also been reported for a calcareous nodule hosting a well preserved crustacean from a nearby section of the Gogo Formation (Melendez et al., 2013a, 2013b). In contrast, other sections of the Gogo Formation which represent the source rocks of the high quality oils in the Canning Basin, have experienced higher thermal maturities (Cadman et al., 1993; Barber et al., 2001; Greenwood and Summons, 2003; Maslen et al., 2009, 2011). Nevertheless, the now exposed or near-surface rocks in most parts of the reef systems in the northern Canning Basin (Lennard Shelf) have likely never been exposed to geological temperatures exceeding 60 to 70 °C (Playford et al., 2009 and references therein).

4.4.1 Preservation of C/N ratios

Fig.5a displays the strong correlation ($R^2 = 0.96$) of total organic nitrogen (TN_{org} %, calculated from TN assuming a constant contribution of $TN_{inorganic}$ of 0.02 %; see below) to total organic carbon (TOC %) and the relatively low C/N values (i.e. TOC/TN_{org}) which suggest these data are representative of the source OM. This would to the best of our knowledge be the oldest reported preservation of C/N source ratios. In (sub)recent sediments

the C/N ratio often provides a reliable distinction of marine *vs*. terrestrial OM since phytoplanktonic organisms typically have a higher nitrogen-content (C/N: ~4-10) than terrestrial vegetation (C/N > 20; (Meyers, 1994, and references therein). However, C/N ratios can be altered by preferential loss of organic nitrogen over organic carbon during diagenesis, leading to artificially high values in affected sediments (e.g. Tyson, 1995, pp. 484-485). Furthermore, C/N data may be corrupted by a contribution of inorganic nitrogen (typically ammonium), particularly in OM-lean sediments (TOC % < 1; e.g. Müller, 1977; Sampei and Matsumoto, 2001). We therefore calculated $TN_{organic}$ % from the measured TN % values by assuming a constant contribution of 0.02% $TN_{inorganic}$ (axis intercept of the TN % *vs.* TOC % plot) and used these corrected values for the determination of C/N ratios (Müller, 1977). The exceptional preservation of C/N ratios in these Palaeozoic sediments is consistent with the excellent preservation of immature OM in some sections of the Gogo Formation.

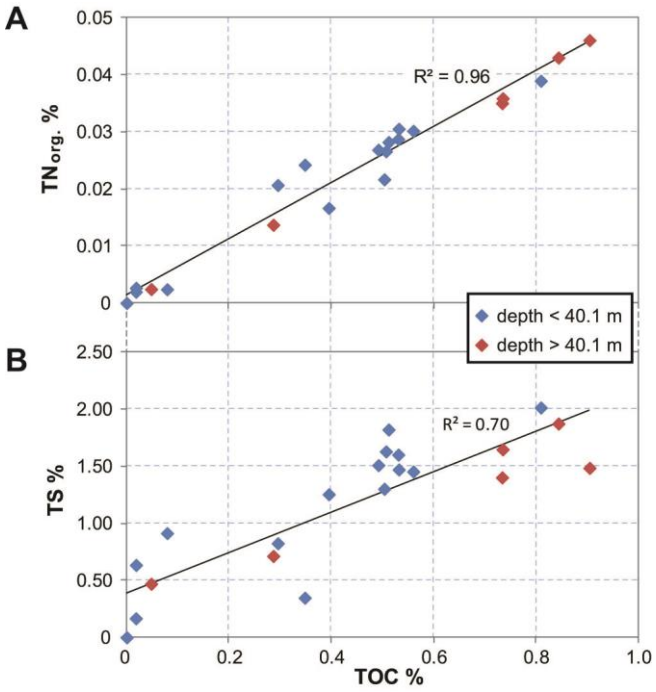

Figure 5: Plots showing positive correlations of total organic carbon (TOC wt. %) to (A) total organic nitrogen (TN_{org} wt. %, corrected from TN % assuming a constant contribution of $TN_{inorganic}$ of 0.02 wt. %) and (B) total sulfur (TS wt. %)

4.4.2 Total organic carbon content (TOC wt. %)

The biomarker data reflected that the degree of thermal alteration was largely independent from the redox conditions at the time of deposition, since all core sections showed similarly low maturity parameters despite the previously discussed strong differences in redox indicators. The estimated original TOC (TOC_{or}, Fig. 6) was calculated according to the following equation developed by Vető et al. (1994).

$$TOC_{or} = TOC + S \times 0.75 \times 1.33$$

This proxy is based on the assumptions that (i) all reduced sulfur was formed syngenetically and (ii) the degradation of OM was essentially due to microbial sulfate reduction (MSR) with the benthic system being more or less closed for dissolved sulfide. The positive correlation between the measured TOC % and TS % (Fig. 5b) may indicate a control of MSR by OM availability. When compared to the relationship established for modern marine sediments (Raiswell and Berner, 1987) all samples have reduced sulfur in excess, which may indicate euxinic conditions, although an overprint by later diagenetic fluids cannot be ruled out. Since the degree of OM alteration is small, there is no indication for a thermally induced change in the C/S ratios (Raiswell and Berner, 1987).

The depth profiles of TOC % and TOC_{or} % are displayed in Fig. 6. Both show slightly higher values in the lower interval which is consistent with enhanced OM preservation under anoxic/euxinic conditions (Claypool and Kaplan, 1974). These data potentially also reflect increased phytoplanktonic productivity compared to the other samples due to enhanced terrigenous nutrient input (section 4.7). However, both, TOC % and TOC_{or} % in these samples are still lower than expected for a palaeoenvironment with prevailing PZE, which may be the result of oligotrophic conditions (despite some terrigenous input), seasonal variability of riverine inflow, anoxia and euxinia or dilution from carbonate precipitation (Tulipani et al., 2014a). The latter is also the presumed reason for the extremely low TOC %

in sediments from the middle interval, where carbonate contents were between 62.6 and 86.2 % (Fig. 6).

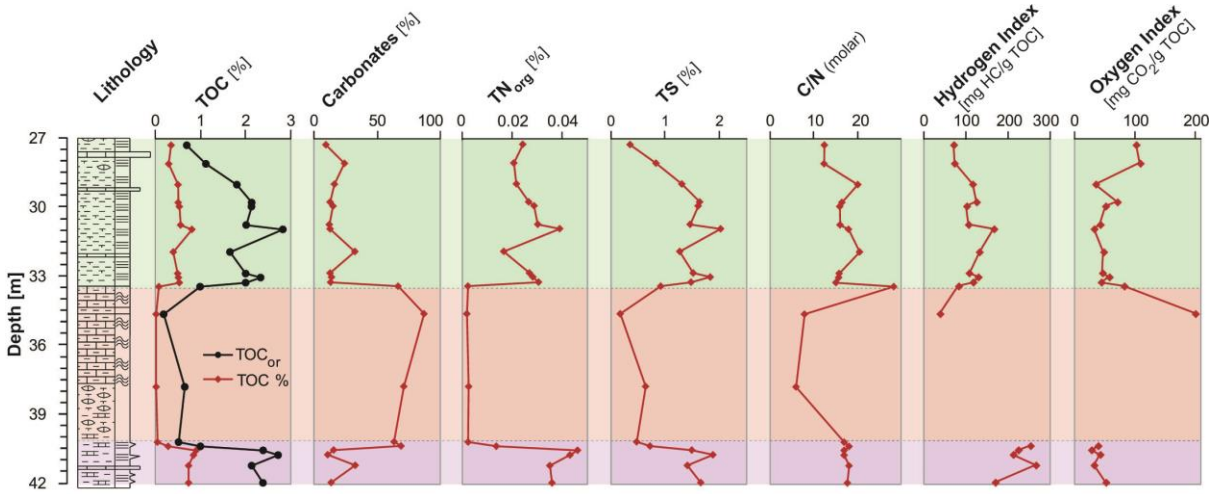

Figure 6: Depth profiles of selected parameters determined by elemental analysis and Rock Eval analysis throughout the MR-1 core. Background colours mark the lower, middle and upper intervals discussed in the text. TOC represents the measured total organic carbon content. TOC_{or} refers to the estimated original TOC in sediments at the time of deposition which was calculated after Vető et al. (1994). TN_{org} = total organic nitrogen content calculated from TN assuming a constant contribution of $TN_{inorganic}$ of 0.02 wt. %. TS = total sulfur content. Data between 33.5-40.1 m have a higher uncertainty due to the very low OM-content. Where gaps in the profiles are shown the determination was not possible due to low TOC.

4.5 Organic matter sources

Whereas the relatively low C/N and C/S signatures (Figs 5 and 6) are suggestive of predominantly marine sourced OM with some terrestrial contribution (Raiswell and Berner, 1987; Meyers, 1994), the high Oxygen Indices (OI) and low Hydrogen Indices (HI) are indicative of Type III kerogens (Fig. 6), which are typically terrigenous (see pseudo van Krevelen diagram in Fig. S5). In some cases Type III kerogens may be derived from oxic or suboxic open marine settings (Peters et al., 2005), which is consistent with the samples deposited later in the Frasnian (middle and upper interval). However, biomarker parameters in the lower interval strongly indicate an anoxic/euxinic marine setting, with some terrigenous input as indicated by land plant spores, recovered from palynological preparations (sections 4.4., 4.6. and 4.7). An increase of HIs and a simultaneous decrease of OIs in this

core interval reflect more reducing conditions, although these values are still not in the range expected for an anoxic marine setting (Fig. S5). Although Rock Eval analysis is a useful screening method, it does have some limitations and can give misleading information about kerogen types due to effects from the mineral matrix, particularly in immature, organic lean samples such as the MR-1 core and typically leads to artificially low HI values (e.g. Katz, 1983; Cowie et al., 1999). Although the samples were decarbonated prior to Rock Eval analysis, matrix effects may have still influenced the results. However, these data could also indicate that periods of persistent water-column stratification accompanied by anoxia and PZE were only episodic or possibly seasonal. This would also be consistent with the presence of some scolecodont fragments (polychaete dentary remains) in these sediments (see section 2.).

4.6 Significance of $\delta^{13}C$ variations

$\delta^{13}C$ values of carbonates, bulk OM and selected hydrocarbons are displayed in Fig. 7. All profiles showed a similar trend of more negative $\delta^{13}C$ values in the lower interval compared to the values between depths of 28.8 and 33.5 m (~2-3 ‰ difference for hydrocarbons and carbonates, ~1 ‰ for bulk OM). Furthermore, $\delta^{13}C$ profiles of bulk OM and hydrocarbons followed a distinctive negative shift in the two uppermost samples (~2 ‰ in OM and ~3 ‰ in hydrocarbons) which were deposited under presumably the most oxic conditions (very high Pr/Ph of ~3). However, this feature was only marginal in the $\delta^{13}C_{carbonate}$ profile. In the lower interval the $\delta^{13}C$ values of carbonates showed some variations which were not observed in the other profiles. $\delta^{13}C$ values in the OM-lean limestone section (middle interval) exhibited pronounced positive shifts, which likely reflect a facies change from the Gogo Formation (basinal) in the lowermost core section to the Sadler Formation (marginal slope). The simultaneous $\delta^{13}C$ shifts in OM and carbonates in

these samples suggest that the $\delta^{13}C$-variations are not caused by diagenetic processes. The low OM-content prevented $\delta^{13}C$ analysis of hydrocarbon in the middle interval.

The similar trends in all $\delta^{13}C$-profiles, with the exception of the excursions in the middle interval, mostly reflect $\delta^{13}C$-variations of the dissolved inorganic carbon (DIC) pool in the palaeowater. The generally more negative $\delta^{13}C$ values in the lower interval, particularly the negative $\delta^{13}C_{carbonate}$ signatures of ~ -3 ‰, may be explained by the "Küspert Model" (Küspert, 1982). In brief, stratification-induced enhanced degradation of ^{13}C-depleted OM in the hypolimnion by SRB led to the accumulation of ^{13}C-depleted DIC in the lower water-column. Some of which diffused into the photic zone where it was recycled by phytoplankton leading to a further ^{13}C depletion of biomass. The fluctuations of $\delta^{13}C_{carbonate}$ in the lower interval may indicate alternation of periods with enhanced recycling of OM (leading to ^{13}C-depletion of DIC) and enhanced burial of ^{13}C-depleted OM (leading to relatively more ^{13}C-enriched OM in sediments).

The negative shift in $\delta^{13}C$ values of OM and hydrocarbons in the two uppermost samples may represent a change in source organisms, since this excursion was only marginal in the $\delta^{13}C$ profile of carbonates. It could also reflect nutrient-poor conditions that contributed to slower growth of phytoplankton, which typically leads to enhanced fractionation against ^{13}C during biosynthesis due to the higher accessibility of $[CO_2]_{aq}$ (i.e. main carbon source; Freeman and Hayes, 1992). This would also be consistent with the lower TOC_{or} % and decreasing biomarker concentrations in these samples (Figs. 3, 6 and 8).

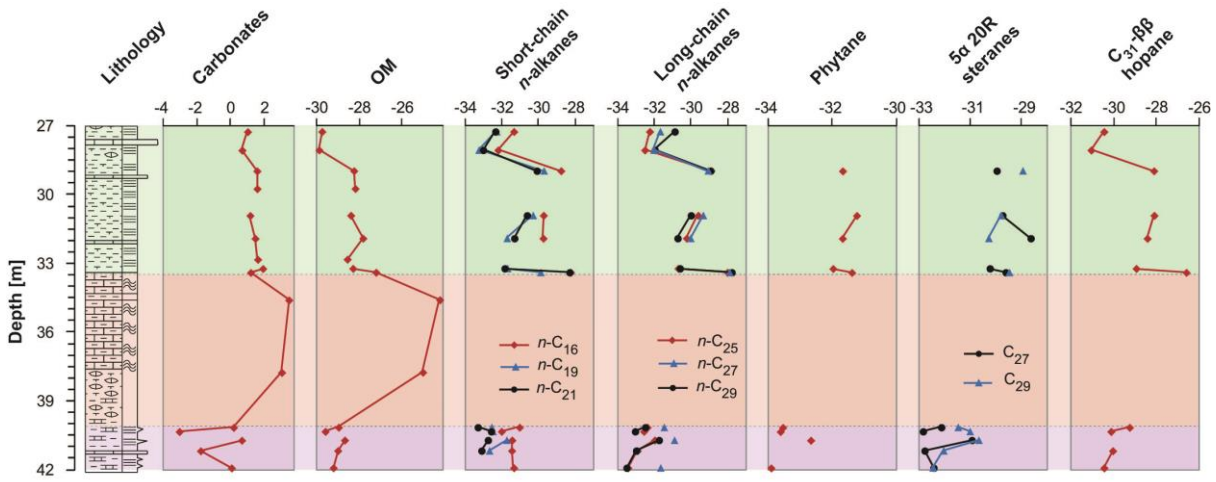

Figure 7: $\delta^{13}C$ depth profiles (reported in ‰ relative to VPDB) throughout the MR-1 core of carbonates, bulk organic matter (OM), representative long- and short-chain *n*-alkanes, phytane, selected regular 5α,14α,17α 20R steranes (5α 20R steranes) and the 17β,21β 22R homohopane (C_{31} ββ hopane). Background colours mark the lower, middle and upper intervals discussed in the text. Where gaps in the profiles are shown, the analyses have only been performed on selected samples or the determination was not possible.

4.7 Changes in populations of primary producers

4.7.1 Variations in steroid and hopanoid distributions

Fig. 8a shows depth profiles of selected molecular parameters which highlight changes in algal and bacterial communities between the setting around the G-F boundary (lower interval) and later in the Frasnian (middle and upper interval). Sterane/hopane ratios were low (< 1) throughout most parts of the upper and middle interval but showed a significant increase in the lower interval, particularly in its upper section. Another notable difference in sediments from the lower interval was the enhanced abundance of 3- and 4-methyl-24 ethylcholestanes. In contrast, the relative abundance of the sponge-specific biomarker 24-*iso*propylcholestane *vs.* 24-*n*-proylcholestane (McCaffrey et al., 1994; Love et al., 2009), which was also displayed in Fig. 8a, did not show significant variations throughout the analysed core (Fig. 8a). Further distinct variations in the lower interval were evident in the

sterane ternary diagram displayed in Fig. 9, which highlights the enhanced relative abundances of C_{27} and C_{28} desmethylsteranes in this core section.

The elevated sterane/hopane ratios in the lower interval are suggestive of a strong predominance of eukaryotic algae over bacteria, whilst the values < 1 in most of the other samples indicate relatively higher bacterial input (e.g. Ourisson et al., 1979; Mackenzie et al., 1982; Brocks et al., 1999). The significantly increased relative abundances of 3- and 4-methyl-24 ethylcholestanes in the lower interval point towards distinct algal communities, possibly as a result of freshwater incursions and water-column stratification. Sedimentary 4-methyl-24 ethylcholestanes are often attributed to dinoflagellates (or their ancestors in Palaeozoic sediments) since they produce a variety of 4-methylsterols (Summons et al., 1987; Goodwin et al., 1988; Summons et al., 1992). However, unlike the dinoflagellate-specific dinosteranes (4,23,24- trimethylcholestanes), 4-methyl-24 ethylcholestanes do have other sources such as marine/brackish prymnesiophyte algae (Volkman et al., 1990). Furthermore, high abundances of 4-methyl-24 ethylcholestanes, particularly in combination with absent or very low-concentrated dinosteranes such as presently detected, have been linked to freshwater settings and attributed to the different algal communities (Summons and Powell, 1987; Fu et al., 1990; Summons et al., 1992). The high abundance of these compounds in sediments from the lower interval deposited around the G-F boundary is therefore coherent with the previously described riverine incursions and algal blooms in the overlying freshwater lens. The $\delta^{13}C$ values of 3- and 4-methyl-24 ethylcholestanes of -29.1 to -32.5 ‰, which could be measured in several samples from the lower interval, are also consistent with a phytoplanktonic source. The covariance of 3β- and 4-methyl-24-ethylcholestanes (Fig. 8a) with similar $\delta^{13}C$ signatures strongly suggests a common source for both product types.

The unusual acritarchs present in the MR-1 core represent a potential source of the 4-methylsteranes. An inferred association of some acritarchs to the cysts of dinoflagellates or

related taxa has been discussed by several authors (Tappan, 1980; Arouri et al., 2000; Moldowan and Talyzina, 1998; Schwark and Empt, 2006; Armstrong and Brasier, 2009).

Changes in algal populations in the lower interval, possibly as a reaction to elevated biotic stress, shallower water depths and anoxia/euxinia, are also reflected by enhanced relative abundances of C_{27} and C_{28} desmethylsteranes in the lower interval (ternary diagram, Fig. 9). Although C_{29} desmethylsteroids are often attributed to a terrestrial origin (e.g. Huang and Meinschein, 1979), here they are probably mainly sourced from green algae (Volkman, 1986, 1998; Kodner et al., 2008; Grosjean et al., 2009), which were likely prominent in the marine Devonian palaeoenvironment.

C_{27} desmethyl steroids are commonly attributed to zooplankton or red algae, but are also produced by some green algae (Kodner et al., 2008; Volkman, 1986). A higher abundance of red algae, which are predominantly macrophytes, would be consistent with shallower water depths at the lower sea-level in the Late Givetian-Early Frasnian. Furthermore, Kelly (2009) suggested the C_{27}/C_{29} sterane ratio in Neoproterozoic-Cambrian sediments was related to palaeoenvironmental redox conditions due to the higher tolerance of red algae to the iron limitation in euxinic environments. Accordingly, higher values of this ratio correlate with euxinic conditions, which is also consistent with the relative increase in C_{27} steroids in the lower interval.

C_{28} desmethylsteroids typically originate from contemporary chlorophyll a and c of algae and prasinophytes and are reported to show elevated abundances in Mesozoic and Cenozoic marine OM (Grantham and Wakefield, 1988; Knoll A.H. et al., 2007). Nevertheless, short term increases of C_{28} steranes relative to C_{29} steranes have been reported in Late Devonian sediments and were attributed to temporary changes in algal populations with higher abundances of prasinophyte algae (Schwark and Empt, 2006), which are well adapted to biotic stress such as oxygen depletion (Tappan, 1980). Ergosterol (C_{28}) is also a

common fungal biomarker (Volkman, 2003) and the co-variation of C_{28} desmethyl sterane abundances and perylene concentrations may be indicative of a common fungal source (section 4.7).

The specific sponge biomarker 24-*iso*propylcholestane (McCaffrey et al., 1994; Love et al., 2009) was present at low abundances throughout the core and most likely originated from demosponges or stromatoporoids (now extinct sponge class), which were together with rugose corals and calcareous microbes the main reef-builders throughout the Devonian until the F-F boundary (e.g. Playford et al., 2009). Although stromatoporoids were amongst the most severely affected organisms in the Late Devonian extinctions (e.g. Fagerstrom, 1994; Playford et al., 2009), potential changes in their abundance is not reflected in the current core-profile of 24-*iso*propylcholestane *vs.* 24-*n*-proylcholestane.

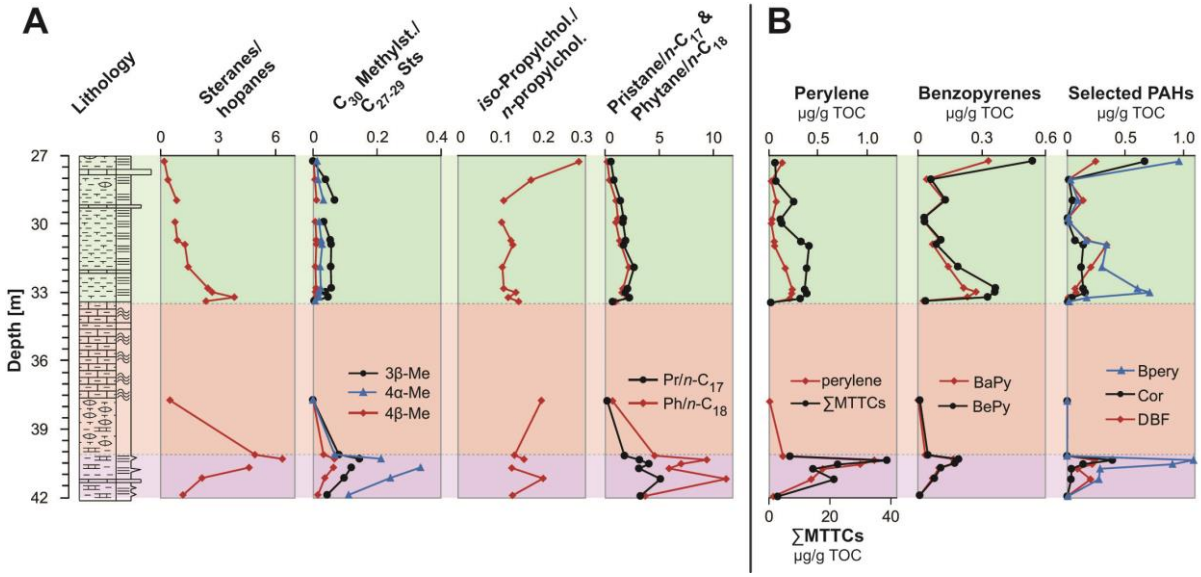

Figure 8: Depth profiles of selected molecular parameters indicative of (A) phytoplankton communities and (B) terrigenous OM-input and combustion sources. Background colours mark the lower, middle and upper intervals discussed in the text. C_{30} Methylst/C_{27-29} Sts = abundance of selected A-ring methylated 24-ethylcholestanes relative to the sum of regular C_{27} – C_{29} 5α14α17α 20R steranes with 3β-Me, 4α-Me and 4β-Me standing for 3β-methyl, 4α-methyl and 4β-methyl -5α14α17α 20R 24-ethylcholestane, respectively. Propylchol. = 24-propylcholestane; Pr = pristane; Ph = phytane; *n*-C_i = *n*-alkane with chain-length "i"; MTTCs = methyltrimethyltridecylchromans; BaPyr = Benzo[*a*]pyrene; BePyr = Benzo[*e*]pyrene; Bpery = Benzo[*ghi*]perylene; Cor = coronene; DBF = dibenzofuran. Where gaps in the profiles are shown, the analyses have only been performed on selected samples or the determination was not possible.

4.7.2 Variations in pristane, phytane and n-alkanes

Distribution, relative abundance and $\delta^{13}C$ values of *n*-alkanes, pristane and phytane often contain valuable information about the palaeoenvironmental algal and bacterial communities as well as higher plant input. Apart from lower abundances of short-chain *n*-alkanes in the OM-lean middle interval, the *n*-alkane distributions showed largely consistent features in parameters such as average chain-length (21.7-23.9) or relative abundances of short-chain *vs.* long-chain lengths throughout the core. The CPI was somewhat decreased in the lower interval and generally slightly higher in *n*-alkanes > C_{22} (Table 1). Furthermore, the ratios of pristane/C_{17} *n*-alkane and phytane/C_{18} *n*-alkane were significantly higher in the lower interval (Fig. 8a). When comparing the $\delta^{13}C$ values displayed in Fig. 7, *n*-alkanes were similar to steranes but slightly more negative than the ββ-20R-homohopane. Furthermore, the $\delta^{13}C$ values of short chain *n*-alkanes were in the same range or slightly more ^{13}C-enriched compared to phytane.

n-Alkanes in sediments with complex marine and terrigenous OM-inputs, such as the presently analysed core, typically have mixed sources including phytoplankton as well as terrestrial and aquatic plants (e.g Collister et al., 1994; Lichtfouse et al., 1994; Tulipani et al., 2014b). The similar or slightly more positive $\delta^{13}C$ values of short chain *n*-alkanes in comparison to the predominantly phytoplankton-derived phytane indicate an origin of these hydrocarbons from phytoplankton as well as possibly heterotrophic bacteria (Tulipani et al., 2014a, and references therein). The generally similar $\delta^{13}C$ signatures of short and long-chain *n*-alkanes in all samples may be indicative of a common source. The slight odd-over-even predominance, which was somewhat more pronounced in *n*-alkanes, > C_{22} (Table 1), is consistent with high algal input (Allard and Templier, 2000; Gelpi et al., 1970; Volkman et al., 1998) and possibly additional contributions, particularly to longer chain-lengths, from aquatic and terrestrial plants (Eglinton and Hamilton, 1967; Ficken et al., 2000). A high algal

contribution to the *n*-alkanes is also supported by the similarity of $\delta^{13}C$ signatures to predominantly algal-derived steranes, whereas the bacterial-derived ββ-20R-homohopane was slightly more ^{13}C-enriched. The decreased CPI in the lower interval (Table 1), despite a presumably higher terrigenous input in this core-section (section 4.7.), was possibly caused by an increased contribution from SRB which are known to produce long-chain *n*-alkanes without an odd-over-even predominance (Davis, 1968; Melendez et al., 2013b). The differences in several of the described *n*-alkane parameters in the OM-lean middle interval are presumably the result of biodegradation after the uplift that followed burial or of diagenesis, with the effects of these magnified in OM-lean horizons.

The increased ratios of pristane/C_{17} *n*-alkane and phytane/C_{18} *n*-alkane in the lower interval may be indicative of significant changes in phytoplankton/algal populations. Similar variations of these ratios, with increased values in OM-richer sediments with evidence of PZE compared to more OM-lean sections have been reported in European Late Devonian (Famennian) sediments (Marynowski and Filipiak, 2007) and were attributed to variations in source organisms. This is also consistent with the previously discussed variations in hopanoid and steroid distributions (section 4.7.1), which similarly reflect significant changes between phytoplankton communities around the G-F boundary and later in the Frasnian.

4.8 Evidence of terrigenous input and combustion sources

Fig. 8b shows the concentration-profiles of total MTTCs and selected 'parent' PAHs (i.e. PAHs lacking alkylation) throughout the MR-1 core. Most PAH profiles showed similar co-variations with highest concentrations in the uppermost sample as well as at depths around 33 m. An exception to this was perylene, which co-varied with chroman abundances and exhibited the highest concentrations in the lower interval. The depth profile of benzo[*ghi*]perylene in the upper part of the core was largely similar to those of most other

PAHs, but it also showed an increase in concentration similar to perylene and MTTCs in the lower interval.

Most sedimentary 'parent' PAHs are products of plant or fossil fuel combustion (Killops and Massoud, 1992; Jiang et al., 1998; Yunker et al., 2002; Grice et al., 2005a, 2007; Nabbefeld et al., 2010c). Their abundance has in some cases also been associated with higher thermal maturities and volcanism (e.g. Murchison and Raymond, 1989). Pyrogenic PAHs often reach sediments *via* airborne particles and their presence in the MR-1 core may be indicative of wildfires. Benzo[*a*]pyrene and coronene are thought to be exclusively formed by pyrogenic processes, whereas other PAHs such as benzo[*e*]pyrene, chrysene or triphenylene may have additional algal sources (Grice et al., 2007; Nabbefeld et al., 2010c). The co-variation of all these PAHs in the MR-1 core strongly implies common combustion sources. Dibenzofuran (**XIX**) has been frequently used as an indicator of higher plant input (Fenton et al., 2007; Nabbefeld et al., 2010c). However, its depth profile in the MR-1 core largely resembled those of the combustion markers (Fig. 8b). Benzo[*ghi*]perylene is typically assigned to a pryogenic origin (Blumer and Youngblood, 1975; Killops and Massoud, 1992), but it has in some cases shown similar sedimentary distributions to perylene (Jiang et al., 1998), implying additional sources of this PAH. In the MR-1 core additional terrigenous sources of benzo[*ghi*]perylene are also likely, particularly in the lower interval.

In contrast to the majority of 'parent' PAHs, perylene has a diagenetic origin and is most likely derived from quinone pigments in wood degrading fungi and therefore presumably linked to terrigenous input (Grice et al., 2009; Jiang et al., 2000; Suzuki et al., 2010). Its covariance with chroman abundances (Fig. 8b) may be indicative of a common terrestrial control, pointing towards enhanced terrigenous OM input *via* riverine inflow in the lower interval (Tulipani et al., 2014a). This would also be consistent with the corresponding slight increase of C/N ratios (Fig. 6).

Further evidence for terrigenous input came from palynological analyses which were performed at core depths between 27.3-29.2 m as well as 38.0-41.7 m (Fig. 1). All of these sediments except the two samples from the organic lean interval (38.0 and 40.1 m) contained comminuted plant debris and plant microfossils, predominantly from the key taxon *Geminospora lemurata* Balme 1962. Whilst these microfossils may be derived from lycopods, a potential origin from progymnosperms has also been suggested due to the resemblance of *G. lemurata* spores to the progymnosperm microspores *Archaeopteris sp.cf. A. jacksonii* Dawson 1862 (Balme, 1995). These were common in coastal floral communities throughout the world during the Middle to early Late Devonian (Balme, 1995). Most samples from 40.4 to 41.7 m (within the lower interval) furthermore contained resin bodies whilst samples between 27.3 to 29.2 m (within the upper interval) often comprised some woody tissue.

4.9 Significance of the present study in the context of other Late Devonian settings in the Canning Basin and globally

In this study we describe significant palaeoenvironmental changes at the location of McWhae Ridge in the Canning Basin between the time periods (i) around the G-F boundary and (ii) later in the Frasnian, with the first representing a distinct time interval of biotic crisis. Depth profiles of redox indicators (Pr/Ph, C_{35} homohopane index, relative abundance of 28,30-DNH) as well as abundances of intact C_{40} *Chlorobi*-carotenoids (Fig. 3) consistently reflect anoxic and photic zone euxinic conditions around the G-F boundary (lower core interval) and a more oxygenated setting later in the Frasnian (upper core interval). This is further corroborated by changes in indicators for water-column stratification and salinity such as the gammacerane index, chroman ratio, $\delta D_{kerogen}$ and $\delta^{18}O_{carbonates}$ (Fig. 3), which indicate (i) a well-mixed water-column later in the Frasnian and (ii) the presence of a stratified water-

column with a freshwater-lens overlying more saline bottom waters near the G-F boundary. Excursions in $\delta^{13}C$ profiles of carbonates, OM and biomarkers in the lower interval (Fig. 7) indicate enhanced recycling of OM in the anoxic sediments/lower water column by sulfate reducing bacteria. These palaeoenvironmental changes also led to distinct algal and bacterial communities at the different time intervals, which are reflected in alterations of steroid and hopanoid distributions, particularly the enhanced abundance of 3- and 4-methyl-24 ethylcholestanes in the lower core interval (Figs. 8a and 9). Furthermore, the simultaneous increase of perylene abundance and chroman ratios in the lower interval (Fig. 8b) suggests terrigenous input, in particular riverine freshwater incursions, which led to the higher nutrient input and development of phytoplankton blooms and associated anoxia/euxinia (Tulipani et al. 2014a).

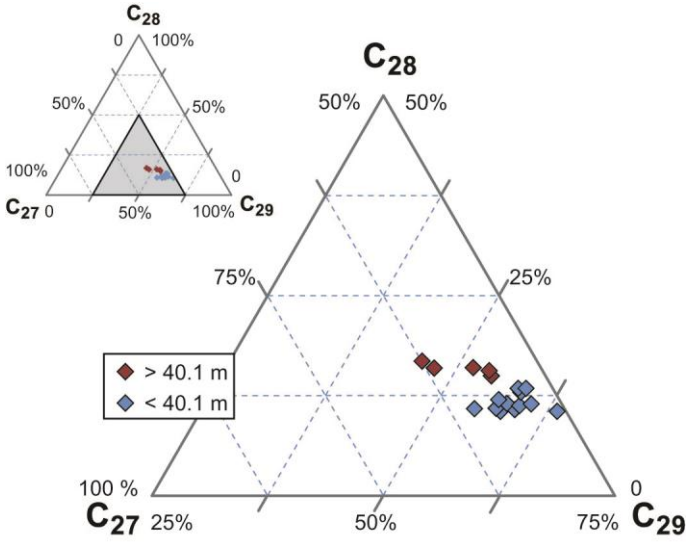

Figure 9: Ternary diagram of regular C_{27} – C_{29} steranes in the MR-1 core. Red diamonds represent samples from a depth > 40.1 m (referred to as lower interval in the text) deposited under anoxic and euxinic conditions and a stagnant, stratified water-column. Blue diamonds represent samples > 40.1 m (referred to as middle and upper interval) presumably deposited under more oxic conditions.

The local scenario around the G-F boundary described here is representative of many marine palaeoenvironments throughout the Middle to Late Devonian since the evolution of

landplants (the first forests of woody plants appeared in the Givetian) is associated with major perturbations in biogeochemical cycling, leading to the development of anoxia and eutrophication in the oceans (e.g. Algeo et al., 1995, 2001; Algeo and Scheckler, 2010; Śliwiński et al., 2011; Tuite and Macko, 2013). Marine anoxia has been reported in many locations particularly at the most severe F-F extinction event (e.g. Joachimski and Buggisch, 1993; Bond et al., 2004; Algeo and Scheckler, 2010; Tuite and Macko, 2013) but also earlier in the Frasnian and Givetian (e.g. House, 2002; Maslen et al., 2009; Śliwiński et al., 2011; Melendez et al., 2013a, 2013b) and has therefore been considered a potential driver for the extinctions. However, in the Canning Basin there is no sedimentological evidence for anoxia at the F-F boundary although the reef systems were severely affected by the extinction event (Becker et al., 1991; George and Chow, 2002; Nothdurft et al., 2004; George et al., 2014). Instead there have been some reports of anoxic or suboxic conditions as well as photic zone euxinia (Maslen et al., 2009; Playford et al., 2009; Melendez et al., 2013a, 2013b) earlier in the Frasnian and Givetian. The present study describes in detail an exemplary setting in the Canning Basin with prevailing anoxia and photic zone euxinia and relates these conditions to terrigenous nutrient input in a distinct time interval around the G-F boundary. The more oxygenated and well mixed watercolumn later in the Frasnian seems consistent with the studies by Becker et al. [1991]; George and Chow [2002] and George et al. [2014], which all report a lack of anoxic facies in the Canning Basin at the F-F boundary. However, the time period of the Latest Frasnian is not covered here due to the low OM content in the corresponding core section.

5. Conclusions and outlook

Organic geochemical characterisation has demonstrated the highly unusual preservation of organic matter in the Gogo Formation of the Canning Basin, including presumably one of

the oldest examples of original C/N preservation. This preservation is enhanced by exceptionally low thermal maturity that is evident in elemental and molecular maturity parameters, and largely unaltered biomarker distributions which included unsaturated hopenes and sterenes.

Furthermore, the organic geochemical data from the Late Givetian-Frasnian core facilitated a detailed reconstruction of the palaeoenvironment over this time period. We found evidence for a distinct time interval of elevated biotic stress, in particular for reef-building organisms and associated fauna, close to or at the G-F boundary, which may represent a local or global extinction event. The palaeoenvironment was characterised by persistent water-column stratification, freshwater incursions, widespread anoxia and enhanced sulfate reduction resulting in the development of persistent anoxia and PZE in the hypolimnion. Elevated concentrations of perylene and MTTCs in sediments from this time interval point towards enhanced terrigenous nutrient input contributing to phytoplankton blooms. The latter commonly represent an important factor in the development of anoxia and PZE, particularly in such a stratified palaeoenvironment. In contrast, sediments deposited later in the Frasnian were presumably laid down under more oxic conditions and a largely well-mixed water-column without particular indications of biotic stress. The abundance of combustion derived PAHs, particularly in the younger sediments, may be indicative of wildfires.

The present study adds to our knowledge of paleoenvironmental conditions associated with the Late Devonian extinctions and might be useful to reconstruct global events if our data can be correlated with other datasets. Furthermore, the correlation of anoxia and PZE with markers of terrigenous input suggests a link between the Middle to Late Devonian extinction events and the rise of higher plants. Our data combined with some previous studies indicate that PZE likely was a significant factor in Middle to Late Devonian extinction events.

Acknowledgements

Geoff Chidlow and Steven Clayton are thanked for technical support with GC-MS and GC-irMS analysis. ST thanks Curtin University for providing a Curtin Strategic International Research Scholarship (CSIRS) and the Institute for Geoscience Research (TiGER) for a top-up scholarship. KG acknowledges the Australian Research Council (ARC) for a Discovery QEII and ARC DORA grant supporting this research, and the John de Laeter Centre for Isotope Research and ARC LIEF grants which provided the infrastructure support. Chevron (Ted Playton), the Geological Survey of Western Australia and the Minerals and Energy Research Institute of Western Australia (M396) are thanked for sponsoring an ARC Linkage grant (LP0883812) which supported the fieldwork and research. All members of this grant are thanked for their contributions. Wundargoodie, Mimbi Community, and Mount Pierre Station are thanked for supporting the field work. MEB wishes to thank P. Escher and I. Scherff, for analytical support. PWH publishes with the permission of the Director, Geological Survey of Western Australia. Research at MIT was supported by a grant from the NASA Astrobiology Institute. Phil Meyers and two unknown reviewers are thanked for their helpful comments.

References

Aboussalam, Z.S., Becker, R.T., 2001. Prospects for an upper Givetian substage. Fossil Record 4, 83-99, doi:10.1002/mmng.20010040107.

Algeo, T.J., Berner, R.A., Maynard, J.B., Scheckler, S.E., 1995. In this Month's issue: Late Devonian Oceanic Anoxic Events and Biotic Crises:" Rooted" in the Evolution of Vascular Land Plants? GSA Today 5, 64-66.

Algeo, T.J., Scheckler, S.E., 2010. Land plant evolution and weathering rate changes in the Devonian. Journal of Earth Science 21, 75-78, doi:10.1007/s12583-010-0173-2.

Algeo, T.J., Scheckler, S.E., Maynard, J.B., 2001. Effects of the Middle to Late Devonian spread of vascular land plants on weathering regimes, marine biotas, and global climate, In: Gensel, P., Edwards, D. (Eds.), Plants invade the land: Evolutionary and environmental perspectives. Columbia University Press, pp. 213-236.

Allard, B., Templier, J., 2000. Comparison of neutral lipid profile of various trilaminar outer cell wall (TLS)-containing microalgae with emphasis on algaenan occurrence. Phytochemistry 54, 369-380, doi:10.1016/s0031-9422(00)00135-7.

Armstrong, H., Brasier, M., 2009. Microfossils. Wiley.

Arouri, K.R., Greenwood, P.F., Walter, M.R., 2000. Biological affinities of Neoproterozoic acritarchs from Australia: microscopic and chemical characterisation. Organic Geochemistry 31, 75-89, doi:http://dx.doi.org/10.1016/S0146-6380(99)00145-X.

Balme, B.E., 1995. Fossil in situ spores and pollen grains: an annotated catalogue. Review of Palaeobotany and Palynology 87, 81-323.

Bambach, R.K., 2006. Phanerozoic biodiversity mass extinctions. Annual Review of Earth and Planetary Sciences 34, 127-155.

Barber, C.J., Grice, K., Bastow, T.P., Alexander, R., Kagi, R.I., 2001. The identification of crocetane in Australian crude oils. Organic Geochemistry 32, 943-947, doi:http://dx.doi.org/10.1016/S0146-6380(01)00057-2.

Barker, C., E., Pawlewicz, M., J., 1994. Calculation of vitrinite reflectance from thermal histories and peak temperatures, Vitrinite Reflectance as a maturity parameter. American Chemical Society, pp. 216-229, doi:10.1021/bk-1994-0570.ch014.

Becker, R.T., House, M.R., Kirchgasser, W.T., Playford, P.E., 1991. Sedimentary and faunal changes across the Frasnian/Famennian boundary in the Canning Basin of Western Australia. Historical Biology 5, 183-196, doi:10.1080/10292389109380400.

Blumer, M., Youngblood, W.W., 1975. Polycyclic Aromatic Hydrocarbons in Soils and Recent Sediments. Science 188, 53-55, doi:10.1126/science.188.4183.53.

Bond, D., Wignall, P.B., Racki, G., 2004. Extent and duration of marine anoxia during the Frasnian–Famennian (Late Devonian) mass extinction in Poland, Germany, Austria and France. Geological Magazine 141, 173-193, doi:10.1017/s0016756804008866.

Böttcher, M.E., Kamyshny, A., Dellwig, O., Farquhar, J., 2012. Multi-isotope biogeochemistry of sulfur in the water column and surface sediments of the Baltic Sea.Geophysical Research Abstracts 14, 2452, .

Böttcher, M.E., Lepland, A., 2000. Biogeochemistry of sulfur in a sediment core from the west-central Baltic Sea: Evidence from stable isotopes and pyrite textures. Journal of Marine Systems 25, 299-312, doi:http://dx.doi.org/10.1016/S0924-7963(00)00023-3.

Brocks, J.J., Logan, G.A., Buick, R., Summons, R.E., 1999. Archean molecular fossils and the early rise of eukaryotes. Science 285, 1033-1036, doi:10.1126/science.285.5430.1033.

Brown, T.C., Kenig, F., 2004. Water column structure during deposition of Middle Devonian-Lower Mississippian black and green/gray shales of the Illinois and Michigan Basins: a biomarker approach. Palaeogeography, Palaeoclimatology, Palaeoecology 215, 59-85, doi:http://dx.doi.org/10.1016/j.palaeo.2004.08.004.

Cadman, S.J., Pain, L., Vuckovic, V., le Poidevin, S.R., 1993. Canning Basin, W.A. Bureau of Resource Sciences, Australian Petroleum Accumulations, Report 9.

Canfield, D.E., Teske, A., 1996. Late Proterozoic rise in atmospheric oxygen concentration inferred from phylogenetic and sulfur-isotope studies. Nature 382, 127-132.

Caplan, M.L., Bustin, R.M., 1999. Devonian-Carboniferous Hangenberg mass extinction event, widespread organic-rich mudrock and anoxia: causes and consequences. Palaeogeography, Palaeoclimatology, Palaeoecology 148, 187-207, doi: http://dx.doi.org/10.1016/S0031-0182(98)00218-1.

Chambers, L.A., Trudinger, P.A., 1979. Microbiological fractionation of stable sulfur isotopes: A review and critique. Geomicrobiology Journal 1, 249-293, doi:10.1080/01490457909377735.

Chen, D., Wang, J., Racki, G., Li, H., Wang, C., Ma, X., Whalen, M.T., 2013. Large sulfur isotopic perturbations and oceanic changes during the Frasnian-Famennian transition of the Late Devonian. Journal of the Geological Society 170, 465-476, doi:10.1144/jgs2012-037.

Claypool, G.E., Kaplan, I.R., 1974. The origin and distribution of methane in marine sediments, in: Kaplan, I.R. (Ed.), Natural gases in marine sediments. Plenum Press, New York, pp. 99-140.

Collister, J.W., Lichtfouse, E., Hieshima, G., Hayes, J.M., 1994. Partial resolution of sources of *n*-alkanes in the saline portion of the Parachute Creek Member, Green River Formation (Piceance Creek Basin, Colorado). Organic Geochemistry 21, 645-659.

Copper, P., 1986. Frasnian/Famennian mass extinction and cold-water oceans. Geology 14, 835-839, doi:10.1130/0091-7613(1986)14<835:fmeaco>2.0.co;2.

Courtillot, V.E., Renne, P.R., 2003. On the ages of flood basalt events. Comptes Rendus Geoscience 335, 113-140, doi:http://dx.doi.org/10.1016/S1631-0713(03)00006-3.

Cowie, G.L., Calvert, S.E., Pedersen, T.F., Schulz, H., von Rad, U., 1999. Organic content and preservational controls in surficial shelf and slope sediments from the Arabian Sea (Pakistan margin). Marine Geology 161, 23-38, doi:http://dx.doi.org/10.1016/S0025-3227(99)00053-5.

Davis, J.B., 1968. Paraffinic hydrocarbons in the sulfate-reducing bacterium *Desulfovibrio desulfuricans*. Chemical Geology 3, 155-160, doi:10.1016/0009-2541(68)90007-7.

Dawson, D., Grice, K., Alexander, R., 2005. Effect of maturation on the indigenous δD signatures of individual hydrocarbons in sediments and crude oils from the Perth Basin (Western Australia). Organic Geochemistry 36, 95-104, doi:10.1016/j.orggeochem.2004.06.020.

Dawson, D., Grice, K., Alexander, R., Edwards, D., 2007. The effect of source and maturity on the stable isotopic compositions of individual hydrocarbons in sediments and crude oils from the

Vulcan Sub-basin, Timor Sea, Northern Australia. Organic Geochemistry 38, 1015-1038, doi:http://dx.doi.org/10.1016/j.orggeochem.2007.02.018.

Dawson, D., Grice, K., Wang, S.X., Alexander, R., Radke, J., 2004. Stable hydrogen isotopic composition of hydrocarbons in torbanites (Late Carboniferous to Late Permian) deposited under various climatic conditions. Organic Geochemistry 35, 189-197, doi:10.1016/j.orggeochem.2003.09.004.

Eglinton, G., Hamilton, R.J., 1967. Leaf epicuticular waxes. Science 156, 1322-1335, doi:10.1126/science.156.3780.1322.

Ellwood, B.B., Benoist, S.L., Hassani, A.E., Wheeler, C., Crick, R.E., 2003. Impact ejecta layer from the Mid-Devonian: possible connection to global mass extinctions. Science 300, 1734-1737, doi:10.1126/science.1081544.

Fagerstrom, J.A., 1994. The history of Devonian-Carboniferous reef communities: Extinctions, effects, recovery. Facies 30, 177-191, doi:10.1007/bf02536896.

Fenton, S., Grice, K., Twitchett, R.J., Böttcher, M.E., Looy, C.V., Nabbefeld, B., 2007. Changes in biomarker abundances and sulfur isotopes of pyrite across the Permian-Triassic (P/Tr) Schuchert Dal section (East Greenland). Earth and Planetary Science Letters 262, 230-239, doi:http://dx.doi.org/10.1016/j.epsl.2007.07.033.

Ficken, K.J., Li, B., Swain, D.L., Eglinton, G., 2000. An *n*-alkane proxy for the sedimentary input of submerged/floating freshwater aquatic macrophytes. Organic Geochemistry 31, 745-749, doi:10.1016/s0146-6380(00)00081-4.

Freeman, K.H., Hayes, J.M., 1992. Fractionation of carbon isotopes by phytoplankton and estimates of ancient CO_2 levels. Global Biogeochemical Cycles 6, 185-198, doi:10.1029/92gb00190.

Fry, B., Jannasch, H.W., Molyneaux, S.J., Wirsen, C.O., Muramoto, J.A., King, S., 1991. Stable isotope studies of the carbon, nitrogen and sulfur cycles in the Black Sea and the Cariaco Trench. Deep Sea Research Part A. Oceanographic Research Papers 38, S1003-S1019, doi:http://dx.doi.org/10.1016/S0198-0149(10)80021-4.

Fu, J., Sheng, G., S., Xu, J., Eglinton, G., Gowar, A.P., Jia, R., Fan, S., F., Peng, P., 1990. Application of biological markers in the assessment of paleoenvironments of Chinese non-marine sediments. Organic Geochemistry 16, 769-779, doi:http://dx.doi.org/10.1016/0146-6380(90)90116-H.

Gat, J.R., 1996. Oxygen and hydrogen isotopes in the hydrologic cycle. Annual Review of Earth and Planetary Sciences 24, 225-262, doi:10.1146/annurev.earth.24.1.225.

Gelpi, E., Schneider, H., Mann, J., Oró, J., 1970. Hydrocarbons of geochemical significance in microscopic algae. Phytochemistry 9, 603-612, doi:10.1016/s0031-9422(00)85700-3.

George, A.D., Chow, N., 2002. The depositional record of the Frasnian/Famennian boundary interval in a fore-reef succession, Canning Basin, Western Australia. Palaeogeography, Palaeoclimatology, Palaeoecology 181, 347-374.

George, A.D., Chow, N., Trinajstic, K.M., 2014. Oxic facies and the Late Devonian mass extinction, Canning Basin, Australia. Geology 42, 327-330.

Goodfellow, W.D., Jonasson, I.R., 1984. Ocean stagnation and ventilation defined by $\delta^{34}S$ secular trends in pyrite and barite, Selwyn Basin, Yukon. Geology 12, 583-586, doi:10.1016/s0031-9422(00)85700-3.

Goodwin, N.S., Mann, A.L., Patience, R.L., 1988. Structure and significance of C_{30} 4-methyl steranes in lacustrine shales and oils. Organic Geochemistry 12, 495-506, doi:http://dx.doi.org/10.1016/0146-6380(88)90159-3.

Grantham, P.J., Wakefield, L.L., 1988. Variations in the sterane carbon number distributions of marine source rock derived crude oils through geological time. Organic Geochemistry 12, 61-73, doi:http://dx.doi.org/10.1016/0146-6380(88)90115-5.

Greenwood, P.F., Summons, R.E., 2003. GC-MS detection and significance of crocetane and pentamethylicosane in sediments and crude oils. Organic Geochemistry 34, 1211-1222, doi:http://dx.doi.org/10.1016/S0146-6380(03)00062-7.

Grey, K., 1992. Miospore asssemblages from the Devonian reef complexes, Canning Basin, Western Australia. Geological Survey of Western Australia, Bulletin 140, 139 pp.

Grice, K., Schaeffer, P., Schwark, L., Maxwell, J.R., 1996. Molecular indicators of palaeoenvironmental conditions in an immature Permian shale (Kupferschiefer, Lower Rhine Basin, north-west Germany) from free and S-bound lipids. Organic Geochemistry 25, 131-147, doi:http://dx.doi.org/10.1016/S0146-6380(96)00130-1.

Grice, K., Schouten, S., Peters, K.E., Sinninghe Damsté, J.S., 1998. Molecular isotopic characterisation of hydrocarbon biomarkers in Palaeocene-Eocene evaporitic, lacustrine source rocks from the Jianghan Basin, China. Organic Geochemistry 29, 1745-1764, doi:.http://dx.doi.org/10.1016/S0146-6380(98)00075-8

Grice, K., Backhouse, J., Alexander, R., Marshall, N., Logan, G.A., 2005a. Correlating terrestrial signatures from biomarker distributions, $\delta^{13}C$, and palynology in fluvio-deltaic deposits from NW Australia (Triassic-Jurassic). Organic Geochemistry 36, doi:1347-1358, doi:http://dx.doi.org/10.1016/j.orggeochem.2005.06.003.

Grice, K., Cao, C., Love, G.D., Böttcher, M.E., Twitchett, R.J., Grosjean, E., Summons, R.E., Turgeon, S.C., Dunning, W., Jin, Y., 2005b. Photic zone euxinia during the Permian-Triassic superanoxic event. Science 307, 706-709, doi:10.1126/science.1104323.

Grice, K., Nabbefeld, B., Maslen, E., 2007. Source and significance of selected polycyclic aromatic hydrocarbons in sediments (Hovea-3 well, Perth Basin, Western Australia) spanning the Permian-Triassic boundary. Organic Geochemistry 38, 1795-1803 doi:http://dx.doi.org/10.1016/j.orggeochem.2007.07.001.

Grice, K., Lu, H., Zhou, Y., Stuart-Williams, H., Farquhar, G.D., 2008. Biosynthetic and environmental effects on the stable carbon isotopic compositions of *anteiso*- (3-methyl) and *iso*-

(2-methyl) alkanes in tobacco leaves. Phytochemistry 69, 2807-2814, doi:10.1016/j.phytochem.2008.08.024.

Grice, K., Lu, H., Atahan, P., Asif, M., Hallmann, C., Greenwood, P., Maslen, E., Tulipani, S., Williford, K., Dodson, J., 2009. New insights into the origin of perylene in geological samples. Geochimica et Cosmochimica Acta 73, 6531-6543, doi:10.1016/j.gca.2009.07.029.

Grosjean, E., Love, G.D., Stalvies, C., Fike, D.A., Summons, R.E., 2009. Origin of petroleum in the Neoproterozoic-Cambrian South Oman Salt Basin. Organic Geochemistry 40, 87-110, doi:http://dx.doi.org/10.1016/j.orggeochem.2008.09.011.

Hartmann, M., Nielsen, H., 2012. $\delta^{34}S$ values in recent sea sediments and their significance using several sediment profiles from the western Baltic Sea. Isotopes in Environmental and Health Studies 48, 7-32, doi:10.1080/10256016.2012.660528.

Harvey, H.R., McManus, G.B., 1991. Marine ciliates as a widespread source of tetrahymanol and hopan-3β-ol in sediments. Geochimica et Cosmochimica Acta 55, 3387-3390.

Hassan, K.M., Spalding, R.F., 2001. Hydrogen isotope values in lacustrine kerogen. Chemical Geology 175, 713-721, doi:http://dx.doi.org/10.1016/S0009-2541(00)00339-9.

House, M.R., 2002. Strength, timing, setting and cause of mid-Palaeozoic extinctions. Palaeogeography, Palaeoclimatology, Palaeoecology 181, 5-25, doi:http://dx.doi.org/10.1016/S0031-0182(01)00471-0.

Huang, W.Y., Meinschein, W.G., 1979. Sterols as ecological indicators. Geochimica et Cosmochimica Acta 43, 739-745, doi:10.1016/0016-7037(79)90257-6.

Hulen, J.B., Collister, J.W., 1999. The oil-bearing, carlin-type gold deposits of Yankee Basin, Alligator Ridge District, Nevada. Economic Geology 94, 1029-1049, doi:10.2113/gsecongeo.94.7.1029.

Jaraula, C.M.B., Grice, K., Twitchett, R.J., Böttcher, M.E., LeMetayer, P., Dastidar, A.G., Opazo, L.F., 2013. Elevated pCO_2 leading to Late Triassic extinction, persistent photic zone euxinia, and rising sea levels. Geology 41, 955-958, doi:10.1130/g34183.1.

Jenkyns, H.C., 2010. Geochemistry of oceanic anoxic events. Geochemistry, Geophysics, Geosystems 11, Q03004, doi:10.1029/2009gc002788.

Jiang, C., Alexander, R., Kagi, R.I., Murray, A.P., 1998. Polycyclic aromatic hydrocarbons in ancient sediments and their relationships to palaeoclimate. Organic Geochemistry 29, 1721-1735, doi:http://dx.doi.org/10.1016/S0146-6380(98)00083-7.

Jiang, C., Alexander, R., Kagi, R.I., Murray, A.P., 2000. Origin of perylene in ancient sediments and its geological significance. Organic Geochemistry 31, 1545-1559, doi:10.1016/s0146-6380(00)00074-7.

Joachimski, M.M., Buggisch, W., 1993. Anoxic events in the late Frasnian-causes of the Frasnian-Famennian faunal crisis? Geology 21, 675-678, doi:10.1130/0091-7613(1993)021<0675:aeitlf>2.3.co;2.

Joachimski, M.M., Ostertag-Henning, C., Pancost, R.D., Strauss, H., Freeman, K.H., Littke, R., Sinninghe Damsté, J.S., Racki, G., 2001. Water column anoxia, enhanced productivity and concomitant changes in $\delta^{13}C$ and $\delta^{34}S$ across the Frasnian-Famennian boundary (Kowala-Holy Cross Mountains/Poland). Chemical Geology 175, 109-131, doi:http://dx.doi.org/10.1016/S0009-2541(00)00365-X.

Jørgensen, B.B., Böttcher, M.E., Lüschen, H., Neretin, L.N., Volkov, I.I., 2004. Anaerobic methane oxidation and a deep H2S sink generate isotopically heavy sulfides in Black Sea sediments. Geochimica et Cosmochimica Acta 68, 2095-2118, doi:http://dx.doi.org/10.1016/j.gca.2003.07.017.

Kampschulte, A., Strauss, H., 2004. The sulfur isotopic evolution of Phanerozoic seawater based on the analysis of structurally substituted sulfate in carbonates. Chemical Geology 204, 255-286, doi:http://dx.doi.org/10.1016/j.chemgeo.2003.11.013.

Kaplan, I.R., Rittenberg, S.C., 1964. Microbiological Fractionation of sulfur isotopes. Journal of General Microbiology 34, 195-212, doi:10.1099/00221287-34-2-195.

Katz, B.J., 1983. Limitations of 'Rock-Eval' pyrolysis for typing organic matter. Organic Geochemistry 4, 195-199, doi:http://dx.doi.org/10.1016/0146-6380(83)90041-4.

Kelly, A.E., 2009. Hydrocarbon biomarkers for biotic and environmental evolution through the Neoproterozoic-Cambrian transition, Massachusetts Institute of Technology, Cambridge, MA.

Killops, S.D., Massoud, M.S., 1992. Polycyclic aromatic hydrocarbons of pyrolytic origin in ancient sediments: evidence for Jurassic vegetation fires. Organic Geochemistry 18, 1-7, doi:http://dx.doi.org/10.1016/0146-6380(92)90137-M.

Klapper, G., 2007. Frasnian (Upper Devonian) conodont succession at Horse Spring and correlative sections, Canning Basin, Western Australia. J. Paleontol. 81, 513-537, doi:10.1666/05088.1.

Knoll A.H., Summons R.E., Waldbauer J.R. 2007. and Zumberge J., The geological succession of primary producers in the oceans. in: Falkowski P., Knoll A.H. (Eds.), The Evolution of Primary Producers in the Sea. Academic Press, Boston, pp. 133–163.

Kodner, R.B., Pearson, A., Summons, R.E., Knoll, A.H., 2008. Sterols in red and green algae: quantification, phylogeny, and relevance for the interpretation of geologic steranes. Geobiology 6, 411-420, doi:10.1111/j.1472-4669.2008.00167.x.

Koopmans, M.P., Schouten, S., Kohnen, M.E.L., Sinninghe Damsté, J.S., 1996. Restricted utility of aryl isoprenoids as indicators for photic zone anoxia. Geochimica et Cosmochimica Acta 60, 4873-4876, doi:http://dx.doi.org/10.1016/S0016-7037(96)00303-1.

Küspert, W., 1982. Environmental changes during oil shale deposition as deduced from stable isotope ratios, in: Einsele, G., Seilacher, A. (Eds.), Cyclic and Event Stratification. Springer, Berlin, pp. 482–501.

Lichtfouse, É., Derenne, S., Mariotti, A., Largeau, C., 1994. Possible algal origin of long chain odd *n*-alkanes in immature sediments as revealed by distributions and carbon isotope ratios. Organic Geochemistry 22, 1023-1027, doi:10.1016/0146-6380(94)90035-3.

Lis, G.P., Schimmelmann, A., Mastalerz, M., 2006. D/H ratios and hydrogen exchangeability of type-II kerogens with increasing thermal maturity. Organic Geochemistry 37, 342-353, doi:http://dx.doi.org/10.1016/j.orggeochem.2005.10.006

Long, J.A., Trinajstic, K., 2010. The Late Devonian Gogo Formation Lägerstatte of Western Australia: Exceptional Early Vertebrate Preservation and Diversity. Annual Review of Earth and Planetary Sciences 38, 255-279 , doi:10.1146/annurev-earth-040809-152416.

Love, G.D., Grosjean, E., Stalvies, C., Fike, D.A., Grotzinger, J.P., Bradley, A.S., Kelly, A.E., Bhatia, M., Meredith, W., Snape, C.E., 2009. Fossil steroids record the appearance of Demospongiae during the Cryogenian period. Nature 457, 718-721, doi:http://www.nature.com/nature/journal/v457/n7230/suppinfo/nature07673_S1.html.

Mackenzie, A.S., Brassell, S.C., Eglinton, G., Maxwell, J.R., 1982. Chemical fossils: the geological fate of steroids. Science 217, 491-504, doi:10.1126/science.217.4559.491.

Marynowski, L., Filipiak, P., 2007. Water column euxinia and wildfire evidence during deposition of the Upper Famennian Hangenberg event horizon from the Holy Cross Mountains (central Poland). Geological Magazine 144, 569-595, doi:10.1017/s0016756807003317.

Marynowski, L., Narkiewicz, M., Grelowski, C., 2000. Biomarkers as environmental indicators in a carbonate complex, example from the Middle to Upper Devonian, Holy Cross Mountains, Poland. Sedimentary Geology 137, 187-212, doi:10.1016/s0037-0738(00)00157-3.

Marynowski, L., Rakociński, M., Borcuch, E., Kremer, B., Schubert, B.A., Jahren, A.H., 2011. Molecular and petrographic indicators of redox conditions and bacterial communities after the F/F mass extinction (Kowala, Holy Cross Mountains, Poland). Palaeogeography, Palaeoclimatology, Palaeoecology 306, 1-14, doi:http://dx.doi.org/10.1016/j.palaeo.2011.03.018.

Maslen, E., Grice, K., Gale, J.D., Hallmann, C., Horsfield, B., 2009. Crocetane: A potential marker of photic zone euxinia in thermally mature sediments and crude oils of Devonian age. Organic Geochemistry 40, 1-11, doi:http://dx.doi.org/10.1016/j.orggeochem.2008.10.005.

Maslen, E., Grice, K., Métayer, P.L., Dawson, D., Edwards, D., 2011. Stable carbon isotopic compositions of individual aromatic hydrocarbons as source and age indicators in oils from western Australian basins. Organic Geochemistry 42, 387-398, doi:http://dx.doi.org/10.1016/j.orggeochem.2011.02.005.

Maslen, E., Grice, K., Dawson, D., Wang, S., Horsfield, B., 2013. Stable hydrogen isotopes for assessing thermal history of sediments through geological time. Thermal history analysis of sedimentary basins: methods and applications. Sedimentary Geology of Mars, SEPM Special Publication No 11, Society of Sedimentary Geology.

McCaffrey, M.A., Michael Moldowan, J., Lipton, P.A., Summons, R.E., Peters, K.E., Jeganathan, A., Watt, D.S., 1994. Paleoenvironmental implications of novel C_{30} steranes in Precambrian to Cenozoic age petroleum and bitumen. Geochimica et Cosmochimica Acta 58, 529-532, doi:http://dx.doi.org/10.1016/0016-7037(94)90481-2.

McGhee, G.R., 1996. The Late Devonian mass extinction. The Frasnian-Famennian crisis. Columbia University Press, New York.

McGhee, G.R., 2005. Modelling Late Devonian extinction hypotheses, in understanding Late Devonian and Permian-Triassic biotic and climatic events-towards an integrated approach, in: Over, J., Morrow, J.R., Wignall, P.G. (Eds.), Developments in paleontology and stratigraphy, no. 20. Elsevier, Amsterdam, pp. 37–50.

McGregor, D.C., Playford, G., 1993. Canadian and Australian Devonian spores: zonation and correlation. Bulletin of the Geological Survey of Canada, v. 438, 125p. (imprinted 1992).

McLaren, D.J., 1970. Time, Life, and Boundaries. Journal of Paleontology 44, 801-815, doi:10.2307/1302714.

McLaren, D.J., 1983. Impacts that changed the course of evolution. New Scientist 100, 588-593.

Melendez, I., Grice, K., Schwark, L., 2013a. Exceptional preservation of Palaeozoic steroids in a diagenetic continuum. Scientific Reports 3. Doi:10.1038/Srep02768.

Melendez, I., Grice, K., Trinajstic, K., Ladjavardi, M., Greenwood, P., Thompson, K., 2013b. Biomarkers reveal the role of photic zone euxinia in exceptional fossil preservation: An organic geochemical perspective. Geology 41, 123-126, doi:10.1130/G33492.1.

Meyers, P.A., 1994. Preservation of elemental and isotopic source identification of sedimentary organic matter. Chemical Geology 114, 289-302, doi:http://dx.doi.org/10.1016/0009-2541(94)90059-0.

Moldowan, J.M., Talyzina, N.M., 1998. Biogeochemical evidence for dinoflagellate ancestors in the Early Cambrian. Science 281, 1168-1170, doi:10.1126/science.281.5380.1168.

Müller, P.J., 1977. C/N ratios in Pacific deep-sea sediments: Effect of inorganic ammonium and organic nitrogen compounds sorbed by clays. Geochimica et Cosmochimica Acta 41, 765-776, doi:http://dx.doi.org/10.1016/0016-7037(77)90047-3.

Murchison, D.G., Raymond, A.C., 1989. Igneous activity and organic maturation in the Midland Valley of Scotland. International Journal of Coal Geology 14, 47-82, doi:http://dx.doi.org/10.1016/0166-5162(89)90078-5.

Murphy, A.E., Sageman, B.B., Hollander, D.J., 2000. Eutrophication by decoupling of the marine biogeochemical cycles of C, N, and P: A mechanism for the Late Devonian mass extinction. Geology 28, 427-430, doi:10.1130/0091-7613(2000)28<427:ebdotm>2.0.co;2.

Nabbefeld, B., Grice, K., Schimmelmann, A., Sauer, P.E., Böttcher, M.E., Twitchett, R., 2010a. Significance of $\delta D_{kerogen}$, $\delta^{13}C_{kerogen}$ and $\delta^{34}S_{pyrite}$ from several Permian/Triassic (P/Tr) sections. Earth and Planetary Science Letters 295, 21-29, doi:http://dx.doi.org/10.1016/j.epsl.2010.03.015.

Nabbefeld, B., Grice, K., Schimmelmann, A., Summons, R.E., Troitzsch, U., Twitchett, R.J., 2010b. A comparison of thermal maturity parameters between freely extracted hydrocarbons (Bitumen I) and a second extract (Bitumen II) from within the kerogen matrix of Permian and Triassic sedimentary rocks. Organic Geochemistry 41, 78-87, doi:http://dx.doi.org/10.1016/j.orggeochem.2009.08.004.

Nabbefeld, B., Grice, K., Summons, R.E., Hays, L.E., Cao, C., 2010c. Significance of polycyclic aromatic hydrocarbons (PAHs) in Permian/Triassic boundary sections. Applied Geochemistry 25, 1374-1382, doi:10.1016/j.apgeochem.2010.06.008.

Nabbefeld, B., Grice, K., Twitchett, R.J., Summons, R.E., Hays, L., Böttcher, M.E., Asif, M., 2010d. An integrated biomarker, isotopic and palaeoenvironmental study through the Late Permian event at Lusitaniadalen, Spitsbergen. Earth and Planetary Science Letters 291, 84-96, doi:http://dx.doi.org/10.1016/j.epsl.2009.12.053.

Neretin, L.N., Böttcher, M.E., Jørgensen, B.B., Volkov, I.I., Lüschen, H., Hilgenfeldt, K., 2004. Pyritization processes and greigite formation in the advancing sulfidization front in the upper Pleistocene sediments of the Black Sea. Geochimica et Cosmochimica Acta 68, 2081-2093, doi:http://dx.doi.org/10.1016/S0016-7037(03)00450-2.

Nothdurft, L.D., Webb, G.E., Kamber, B.S., 2004. Rare earth element geochemistry of Late Devonian reefal carbonates, Canning Basin, Western Australia: confirmation of a seawater REE proxy in ancient limestones. Geochimica et Cosmochimica Acta 68, 263-283, doi: http://dx.doi.org/10.1016/S0016-7037(03)00422-8

Obermajer, M., Fowler, M.G., Snowdon, L.R., Macqueen, R.W., 2000. Compositional variability of crude oils and source kerogen in the Silurian carbonate-evaporite sequences of the eastern Michigan Basin, Ontario, Canada. Bulletin of Canadian Petroleum Geology 48, 307-322, doi:10.2113/48.4.307.

Ourisson, G., Albrecht, P., Rohmer, M., 1979. Hopanoids-paleochemistry and biochemistry of a group of natural products. Pure and Applied Chemistry 51, 709-729.

Pedentchouk, N., Freeman, K.H., Harris, N.B., 2006. Different response of δD values of *n*-alkanes, isoprenoids, and kerogen during thermal maturation. Geochimica et Cosmochimica Acta 70, 2063-2072, doi:http://dx.doi.org/10.1016/j.gca.2006.01.013.

Peters, K.E., Moldowan, J.M., 1991. Effects of source, thermal maturity, and biodegradation on the distribution and isomerization of homohopanes in petroleum. Organic Geochemistry 17, 47-61, doi:http://dx.doi.org/10.1016/0146-6380(91)90039-M.

Peters, K.E., Walters, C.C., Moldowan, J.M., 2005. The biomarker guide: Interpreting molecular fossils in petroleum and ancient sediments. Prentice-Hall, New Jersey.

Playford, P.E., Hocking, R.M., Cockbain, A.E., 2009. Devonian reef complexes of the Canning Basin, Western Australia: Geological Survey of Western Australia, Bulletin 145, 444p.

Polissar, P.J., Freeman, K.H., 2010. Effects of aridity and vegetation on plant-wax δD in modern lake sediments. Geochimica et Cosmochimica Acta 74, 5785-5797, doi:10.1016/j.gca.2010.06.018.

Quandt, L., Gottschalk, G., Ziegler, H., Stichler, W., 1977. Isotope discrimination by photosynthetic bacteria. FEMS Microbiology Letters 1, 125-128, doi:10.1111/j.1574-6968.1977.tb00596.x.

Racki, G., 2005. Toward understanding Late Devonian global events: few answers, many questions, in understanding Late Devonian and Permian-Triassic biotic and climatic events-towards an integrated approach in: Over, D.J., Morrow, J.R., Wignall, P.B. (Eds.), Developments in paleontology and stratigraphy, no. 20. Elsevier, Amsterdam, pp. 5–36.

Raiswell, R., Berner, R.A., 1987. Organic carbon losses during burial and thermal maturation of normal marine shales. Geology 15, 853-856, doi:10.1130/0091-7613(1987)15<853:ocldba>2.0.co;2.

Requejo, A.G., Allan, J., Creaney, S., Gray, N.R., Cole, K.S., 1992. Aryl isoprenoids and diaromatic carotenoids in Paleozoic source rocks and oils from the Western Canada and Williston Basins. Organic Geochemistry 19, 245-264, doi:http://dx.doi.org/10.1016/0146-6380(92)90041-U.

Sachse, D., Radke, J., Gaupp, R., Schwark, L., Lüniger, G., Gleixner, G., 2004. Reconstruction of palaeohydrological conditions in a lagoon during the 2nd Zechstein cycle through simultaneous use of δD values of individual n-alkanes and $\delta^{18}O$ and $\delta^{13}C$ values of carbonates. International Journal of Earth Sciences (Geologische Rundschau) 93, 554-564, doi:10.1007/s00531-004-0408-5.

Sampei, Y., Matsumoto, E., 2001. C/N ratios in a sediment core from Nakaumi Lagoon, southwest Japan -usefulness as an organic source indicator-. Geochemical Journal 35, 189-205.

Sandberg, C.A., Morrow, J.R., Ziegler, W., 2002. Late Devonian sea-level changes, catastrophic events, and mass extinctions, in: Koeberl, C., MacLeod, K.G. (Eds.), Catastrophic events and mass extinctions: Impacts and beyond. Geological Society of America Special Paper, Boulder, Colorado, pp. 473-487.

Schimmelmann, A., 1991. Determination of the concentration and stable isotopic composition of nonexchangeable hydrogen in organic matter. Analytical Chemistry 63, 2456-2459, doi:10.1021/ac00021a013.

Schimmelmann, A., Lewan, M.D., Wintsch, R.P., 1999. D/H isotope ratios of kerogen, bitumen, oil, and water in hydrous pyrolysis of source rocks containing kerogen types I, II, IIS, and III. Geochimica et Cosmochimica Acta 63, 3751-3766,10.1016/s0016-7037(99)00221-5.

Schimmelmann, A., Sessions, A.L., Mastalerz, M., 2006. Hydrogen isotopic (D/H) composition of organic matter during diagenesis and thermal maturation. Annual Review of Earth and Planetary Sciences 34, 501-533.

Schwark, L., Empt, P., 2006. Sterane biomarkers as indicators of palaeozoic algal evolution and extinction events. Palaeogeography, Palaeoclimatology, Palaeoecology 240, 225-236, doi:http://dx.doi.org/10.1016/j.palaeo.2006.03.050.

Schwark, L., Frimmel, A., 2004. Chemostratigraphy of the Posidonia Black Shale, SW-Germany: II. Assessment of extent and persistence of photic-zone anoxia using aryl isoprenoid distributions. Chemical Geology 206, 231-248, doi:http://dx.doi.org/10.1016/j.chemgeo.2003.12.008.

Schwark, L., Vliex, M., Schaeffer, P., 1998. Geochemical characterization of Malm Zeta laminated carbonates from the Franconian Alb, SW-Germany (II). Organic Geochemistry 29, 1921-1952, doi:http://dx.doi.org/10.1016/S0146-6380(98)00192-2.

Sepkoski, J.J., 1986. Phanerozoic overview of mass extinction, in: Raup, D.M., Jablonski, D. (Eds.), Patterns and Processes in the History of Life. Springer Verlag, Berlin, pp. 277–295

Sepkoski, J.J., Jr., 1993. Ten years in the library: new data confirm paleontological patterns. Paleobiology 19, 43-51, doi:10.2307/2400770.

Sessions, A.L., Burgoyne, T.W., Schimmelmann, A., Hayes, J.M., 1999. Fractionation of hydrogen isotopes in lipid biosynthesis. Organic Geochemistry 30, 1193-1200, doi:10.1016/s0146-6380(99)00094-7.

Sim, M.S., Bosak, T., Ono, S., 2011. Large sulfur isotope fractionation does not require disproportionation. Science 333, 74-77, doi:10.1126/science.1205103.

Sinninghe Damsté, J.S., Kock-Van Dalen, A.C., De Leeuw, J.W., Schenck, P.A., Guoying, S., Brassell, S.C., 1987. The identification of mono-, di- and trimethyl 2-methyl-2-(4,8,12-trimethyltridecyl)chromans and their occurrence in the geosphere. Geochimica et Cosmochimica Acta 51, 2393-2400, doi:http://dx.doi.org/10.1016/0016-7037(87)90292-4.

Sinninghe Damsté, J.S., Kenig, F., Koopmans, M.P., Köster, J., Schouten, S., Hayes, J.M., de Leeuw, J.W., 1995. Evidence for gammacerane as an indicator of water column stratification. Geochimica et Cosmochimica Acta 59, 1895-1900, doi:http://dx.doi.org/10.1016/0016-7037(95)00073-9.

Sirevåg, R., Buchanan, B.B., Berry, J.A., Troughton, J.H., 1977. Mechanisms of CO_2 fixation in bacterial photosynthesis studied by the carbon isotope fractionation technique. Archives of Microbiology 112, 35-38, doi:10.1007/bf00446651.

Śliwiński, M.G., Whalen, M.T., Newberry, R.J., Payne, J.H., Day, J.E., 2011. Stable isotope ($\delta^{13}C_{carb\ and\ org}$, $\delta^{15}N_{org}$) and trace element anomalies during the Late Devonian 'punctata Event' in the Western Canada Sedimentary Basin. Palaeogeography, Palaeoclimatology, Palaeoecology 307, 245-271.

Staplin, F.L., 1969. Sedimentary organic matter, organic metamorphism, and oil and gas occurrence. Bulletin of Canadian Petroleum Geology 17, 47-66.

Summons, R.E., Powell, T.G., 1986. Chlorobiaceae in Palaeozoic seas revealed by biological markers, isotopes and geology. Nature 319, 763-765.

Summons, R.E., Powell, T.G., 1987. Identification of aryl isoprenoids in source rocks and crude oils: Biological markers for the green sulphur bacteria. Geochimica et Cosmochimica Acta 51, 557-566, doi:http://dx.doi.org/10.1016/0016-7037(87)90069-X.

Summons, R.E., Volkman, J.K., Boreham, C.J., 1987. Dinosterane and other steroidal hydrocarbons of dinoflagellate origin in sediments and petroleum. Geochimica et Cosmochimica Acta 51, 3075-3082, doi:http://dx.doi.org/10.1016/0016-7037(87)90381-4.

Summons, R.E., Thomas, J., Maxwell, J.R., Boreham, C.J., 1992. Secular and environmental constraints on the occurrence of dinosterane in sediments. Geochimica et Cosmochimica Acta 56, 2437-2444, doi:http://dx.doi.org/10.1016/0016-7037(92)90200-3.

Summons, R.E., Love, G.D., Hays, L., Cao, C., Jin, Y., Shen, S.Z., Grice, K., Foster, C.B., 2006. Molecular evidence for prolonged photic zone euxinia at the Meishan and East Greenland sections of the Permian Triassic Boundary. Geochimica et Cosmochimica Acta 70, A625, doi:http://dx.doi.org/10.1016/j.gca.2006.06.1159.

Suzuki, N., Yessalina, S., Kikuchi, T., 2010. Probable fungal origin of perylene in Late Cretaceous to Paleogene terrestrial sedimentary rocks of northeastern Japan as indicated from stable carbon isotopes. Organic Geochemistry 41, 234-241, doi:10.1016/j.orggeochem.2009.11.010.

Tappan, H.N., 1980. The paleobiology of plant protists. WH Freeman San Francisco.

ten Haven, H.L., De Leeuw, J.W., Schenck, P.A., 1985. Organic geochemical studies of a Messinian evaporitic basin, northern Apennines (Italy) I: Hydrocarbon biological markers for a hypersaline environment. Geochimica et Cosmochimica Acta 49, 2181-2191, doi:10.1016/0016-7037(85)90075-4.

Tuite, M.L., Macko, S.A., 2013. Basinward nitrogen limitation demonstrates role of terrestrial nitrogen and redox control of $\delta^{15}N$ in a Late Devonian black shale. Geology 41, 1079-1082.

Tulipani, S., Grice, K., Greenwood, P., Schwark, L., Böttcher, M.E., Summons, R.E., Foster, C.B., 2014a. Molecular proxies as indicators of freshwater incursion-driven salinity stratification. Geochemistry, Geophysics, Geosystems. in review.

Tulipani, S., Grice, K., Krull, E., Greenwood, P., A.T., R., 2014b. Salinity variations in the Northern Coorong Lagoon, South Australia: Significant changes in the Ecosystem following human alteration to the natural water regime. Organic Geochemistry 75, 74-86.

Tyson, R., 1995. Sedimentary organic matter. 615 pp. Chapman & Hall, London.

Vető, I., Hetényi, M., Demény, A., Hertelendi, E., 1994. Hydrogen index as reflecting intensity of sulfidic diagenesis in non-bioturbated, shaly sediments. Organic Geochemistry 22, 299-310, doi:http://dx.doi.org/10.1016/0146-6380(94)90176-7.

Volkman, J.K., 1986. A review of sterol markers for marine and terrigenous organic matter. Organic Geochemistry 9, 83-99, doi:10.1016/0146-6380(86)90089-6.

Volkman, J.K., 2003. Sterols in microorganisms. Applied Microbiology and Biotechnology 60, 495-506, doi:10.1007/s00253-002-1172-8.

Volkman, J.K., Kearney, P., Jeffrey, S.W., 1990. A new source of 4-methyl sterols and 5α(H)-stanols in sediments: prymnesiophyte microalgae of the genus Pavlova. Organic Geochemistry 15, 489-497, doi:http://dx.doi.org/10.1016/0146-6380(90)90094-G.

Volkman, J.K., Barrett, S.M., Blackburn, S.I., Mansour, M.P., Sikes, E.L., Gelin, F., 1998. Microalgal biomarkers: a review of recent research developments. Organic Geochemistry 29, 1163-1179, doi:10.1016/s0146-6380(98)00062-x.

Walliser, O.H., 1996. Global events in the Devonian and Carboniferous, in: Walliser, O.H. (Ed.), Global events and event stratigraphy in the Phanerozoic. Springer-Verlag Berlin Heidelberg New York, pp. 225-250.

Wortmann, U.G., Paytan, A., 2012. Rapid variability of seawater chemistry over the past 130 million years. Science 337, 334-336, doi:10.1126/science.1220656.

Yunker, M.B., Macdonald, R.W., Vingarzan, R., Mitchell, R.H., Goyette, D., Sylvestre, S., 2002. PAHs in the Fraser River basin: a critical appraisal of PAH ratios as indicators of PAH source and composition. Organic Geochemistry 33, 489-515, doi:http://dx.doi.org/10.1016/S0146-6380(02)00002-5.

Zhou, Y., Grice, K., Chikaraishi, Y., Stuart-Williams, H., Farquhar, G.D., Ohkouchi, N., 2011. Temperature effect on leaf water deuterium enrichment and isotopic fractionation during leaf lipid biosynthesis: Results from controlled growth of C3 and C4 land plants. Phytochemistry 72, 207-213, doi:10.1016/j.phytochem.2010.10.022.

Ziebis, W., Böttcher, M.E., Weber, A., Miquel, J.-C., Sievert, S., Linke, P., 2000. Bacterial sulfate reduction and sulfur isotope discrimination in the hypersaline and hypersulfidic water column of the Urania Basin (Mediterranean Sea), Journal of Conference Abstracts, 5, 1134.

Supplementary material

Experimental

If not indicated otherwise, all analyses were performed in the laboratory of WA-OIGC at Curtin University. All glassware used was annealed at 550 °C for 1 hour and procedural blanks were run regularly. Most of the methods have been described in Tulipani et al. (2014), but summaries of these are also included below.

Sample collection, preparation and extraction

The core was collected without any drilling fluids or lubricants using a small portable drilling rig. Samples were cut with a rocksaw (diamond crystal edge with carbon steel centre) and pre-extracted in methanol and dichloromethane (DCM) in an ultrasonic bath to remove any potential surface contamination. Samples were ground in a stainless-steel rock-mill and Soxhlet extracted with DCM/methanol 9:1 v/v for 48 hours. Activated copper turnings were used for the removal of elemental sulfur. The extracts were further separated by silica gel-column chromatography using solvents with an increasing polarity. Aliphatic and aromatic fractions were eluted in hexane/DCM 5:1 v/v, respectively. Samples for palynological analyses were not identical to the larger samples for biomarker, elemental and isotope analysis and represented small chips taken throughout the core.

Gas-chromatography-mass spectrometry (GC-MS)

The analyses were performed on an Agilent 5973 Mass-Selective Detector (MSD) interfaced to an Agilent 6890 gas chromatograph (GC) fitted with an autosampler, utilizing a DB-5MS capillary column (60 m × 0.25 mm I.D.,0.25 μm film thickness; J & W scientific). The GC-oven was typically heated up from 40 °C to 310 °C (aliphatic fractions) or 325 °C (aromatic fractions) at 3 °C/min with initial and final hold times of 1 and 30 minutes, respectively. Samples were injected into a split/splitless injector at 320 °C in a pulsed-splitless mode. The carrier gas (helium) flow rate was kept constant at 1.1 mL/min. Full scan (50 - 550 Daltons) at 70 eV mass spectra and selected ion monitoring (SIM) spectra (used for quantification of aromatic compounds) were typically acquired with an electron multiplier voltage of 1800 V and a source temperature of 230 °C. ChemStation Data Analysis software was used for data acquisition and processing. Perylene, palaeorenieratane and isorenieratane were identified by comparison of retention times and mass spectra with authentic standards.

For semi-quantitative analyses without consideration of response factors the aromatic fractions were spiked with a known amount of perdeuterated terphenyl (d^{14}).

Multiple reaction monitoring (MRM) GC-MS

The analyses were performed at MIT on a Micromass Autospec Ultima mass spectrometer interfaced to an Agilent 6890 N gas chromatograph fitted with an autosampler and a DB-5MS capillary column (60 m×0.25 mm I.D.; 0.25 μm film thickness; J&W Scientific). The carrier gas (helium) flow rate was kept constant at 2 mL/min. The GC-oven was programmed from 60 °C to 150 °C at 10 °C/min and to 315 °C at 3 °C/min with initial and final hold times of 2 and 24 min, respectively. The source was operated in electron impact (EI, 70 eV) mode at 250 °C, with 8 kV accelerating voltage. Data were acquired and processed using MassLynx 4.0 (Micromass Ltd.) software. Identification of compounds was achieved by comparison with a synthetic mixture of oils (AGSO standard) that contains most common hopanes and steranes. Semi quantitative analyses were achieved by spiking the samples with a known amount of perdeuterated (d^4) 24-ethylcholestane. The transitions of precursor-product reactions used to monitor the compounds relevant for this study are included in Figs. 2, 3, and 5.

Compound specific-stable isotope analysis

A Micromass IsoPrime mass-spectrometer interfaced to an Agilent 6890N GC fitted with an autosampler was utilized with GC- column, carrier gas, injector conditions and oven temperature programs identical to the settings for GC-MS analysis. The interface for the conversion of analytes to CO_2 and H_2O consisted of a quartz tube packed with CuO-pellets (4 mm x 0.5 mm, isotope grade, Elemental Microanalysis LTD.) and was maintained at 850 °C. H_2O was removed cryogenically at -100 °C. Isotopic compositions were determined by integration of the *m/z* 44, 45 and 46 ion currents of CO_2 peaks from each analyte and reported relative to CO_2 reference gas pulses of known ^{13}C-content. Isotopic values are given in the delta (δ) notation relative to VPDB. For data acquisition and processing MassLynx (Micromass Ltd.) was used. Each sample was analysed at least in duplicate and all reported values had standard deviations < 0.5 ‰. To ensure accuracy, in-house standard solutions containing *n*-alkanes with a known isotopic composition were analysed after every second sample.

Elemental analysis

Elemental analysis (C, N, S) was performed in the laboratory of the Institute of Geoscience, Kiel University. Prior to analysis, fractions of the ground samples were decarbonated with hydrochloric acid (5%), washed, dried and homogenized. The carbonate content [wt. %] was calculated based on weight differences before and after decarbonation. The reported values for TOC %, TN % and TS % have also been corrected for these weight differences. Analyses were performed on a VARIO EL-III elemental analyser. About every second sample was analysed in duplicate or triplicate to ensure reproducibility.

Rock Eval analysis

Rock Eval analysis was performed in the laboratory of the Institute of Geoscience, Kiel University on fractions of the decarbonated samples (previous section) using a VINCI Rock Eval 2 instrument.

$\delta^{13}C$ and $\delta^{18}O$ of carbonates

$\delta^{13}C$ and $\delta^{18}O$ of carbonates were measured in the laboratory of the School of Plant Biology at the University of Western Australia by continuous flow (CF) analysis using a GasBench II coupled with a Delta XL Mass Spectrometer (Thermo-Fisher Scientific) after the method described in Paul and Skrzypek (2007). In brief, carbonates in the powdered samples were digested by addition of anhydrous ortho-phosphoric acid in a helium atmosphere. The generated CO_2 was trapped, purified and diverted to the irMS. Isotope values were reported in the delta (δ) notation relative to VPDB.

$\delta^{13}C$ of organic carbon

$\delta^{13}C$ of organic carbon was measured in the laboratory of the School of Plant Biology at the University of Western Australia. Residues left after Soxhlet extraction were treated with ~7M hydrochloric acid to remove carbonates, washed, dried and homogenized. $\delta^{13}C$ analyses were subsequently performed on a continuous flow (CF) system consisting of a Delta V Plus mass spectrometer connected to a Thermo Flush 1112 *via* Conflo IV (Thermo-Fisher Scientific) after the method described in Skrzypek and Paul (2006). The combustion and oxidation temperatures were 1700-1800 °C, the reduction temperature 650 °C. Results were reported in the delta (δ) notation relative to VPDB.

$\delta^{34}S$ of pyrite

$\delta^{34}S$ of total reducable inorganic sulfur (TRIS, basically pyrite) was measured at the Geochemistry & Isotope Geochemistry Group, Marine Geology Department, Leibniz-Institute for Baltic Sea Research in a fraction of the sample residue after Soxhlet-extraction. Instrumentation and methods have been described in Tulipani et al. (2014). In brief, TRIS was extracted from the sample by treatment with hot acidic chromium (II) chloride (Fossing & Jørgensen, 1989) and the generated H_2S was precipitated as ZnS and subsequently converted to AgS_2. $^{34}S/^{32}S$ ratios were measured by combustion - isotope ratio mass spectrometry (C-irMS) on a Thermo Finnigan MAT 253 mass spectrometer coupled to an elemental analyser (Thermo Flash 2000) *via* a split interface (Thermo Finnigan Conflo IV). Measured isotope ratios were calibrated with in-house and international reference materials (Mann et al., 2009) and reported in the δ-notation relative to V-CDT (Vienna Cañon Diablo Troilite).

δD of kerogen

δD of kerogen was measured at the Department of Geological Sciences, Indiana University. Kerogens were isolated from the extracted residue by decarbonation with ~7M hydrochloric acid and a subsequent treatment with 25 % hydrofluoric acid to remove silicates and other hydrogen-bearing inorganic phases. Heavy minerals such as acid-insoluble sulfides, titanium oxides and zircon were removed from the kerogen by density separation using aqueous zinc bromide solution (~2.4 g/mL). Zinc bromide was subsequently removed by washing with slightly acidified water. Samples were freeze dried and extracted ultrasonically in DCM for 2 hours to remove any bitumen previously trapped in the mineral matrix. After washing with DCM, drying and homogenization the kerogens were weighed into silver capsules for δD analysis.

δD analyses of the kerogens were performed according to the method described by Sauer et al. (2009). To account for exchangeable hydrogen, aliquots of the kerogens (2 replicates each) were equilibrated in two different water vapours with known δD values at 115 °C for at least 6 h prior to analysis. δD analyses were performed using a Thermo Finnigan thermal conversion elemental analyser (TC/EA) coupled to a Thermo Finnigan Delta Plus XP isotope ratio mass spectrometer which was operated in continuous-flow mode. The contents of exchangeable hydrogen were determined using mass balance equations and the measured δD values were corrected accordingly (Schimmelmann et al., 1999, 2006).

Palynological analyses

Palynological analyses were performed at Geoscience Australia Kerogens were examined with standard palynological techniques (Wood et al. 1996). Unoxidised, unfiltered, kerogen slides were prepared, and when required the kerogen was oxidised and filtered (10µm) to produce strew slides examined in this study.

Supplementary figures

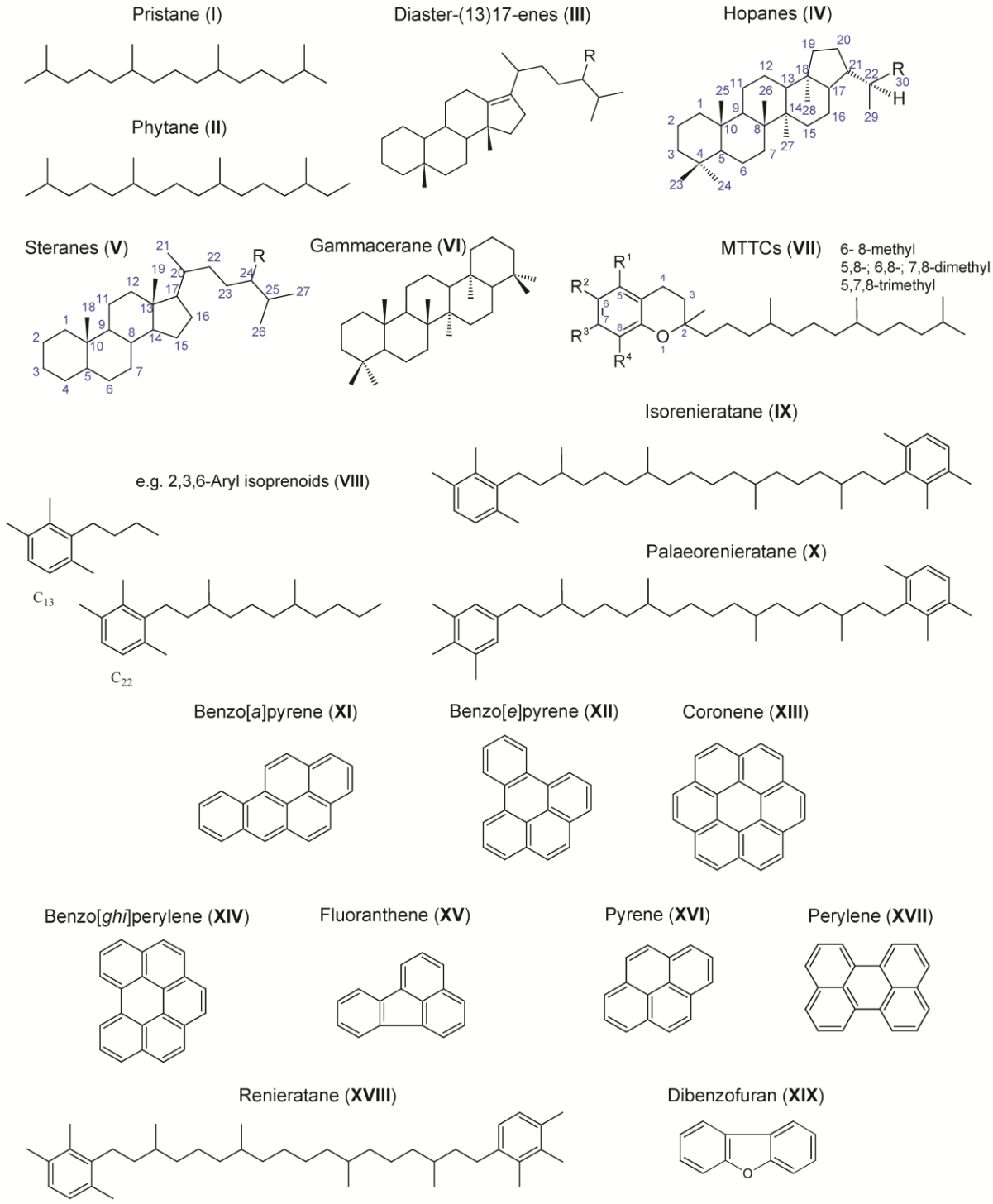

Figure S1: Structures referred to in the text.

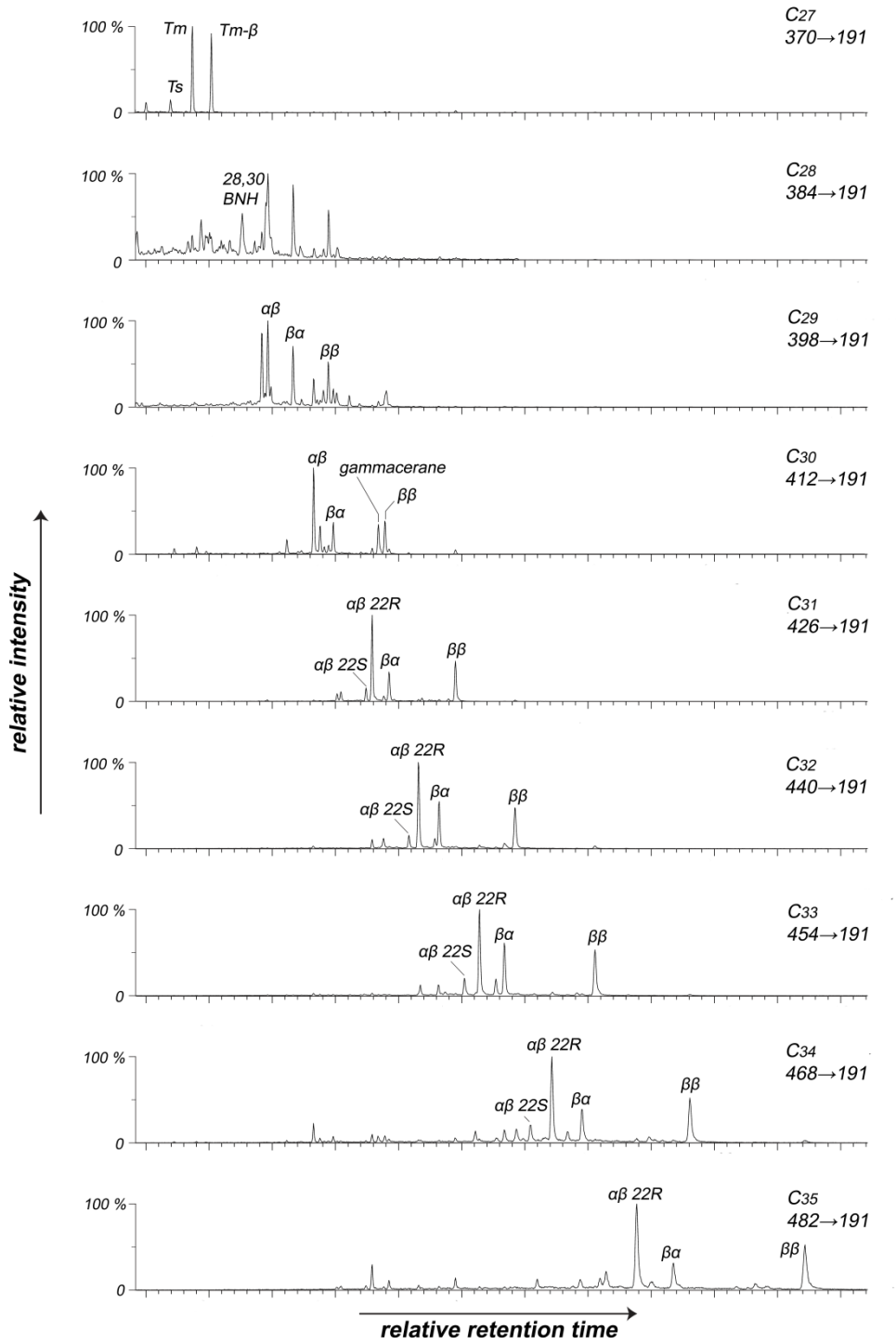

Figure S2: MRM chromatograms showing hopanes in a sample from the analysed core at the depth of 40.7 m. S and R stand for the stereochemistry at C22.

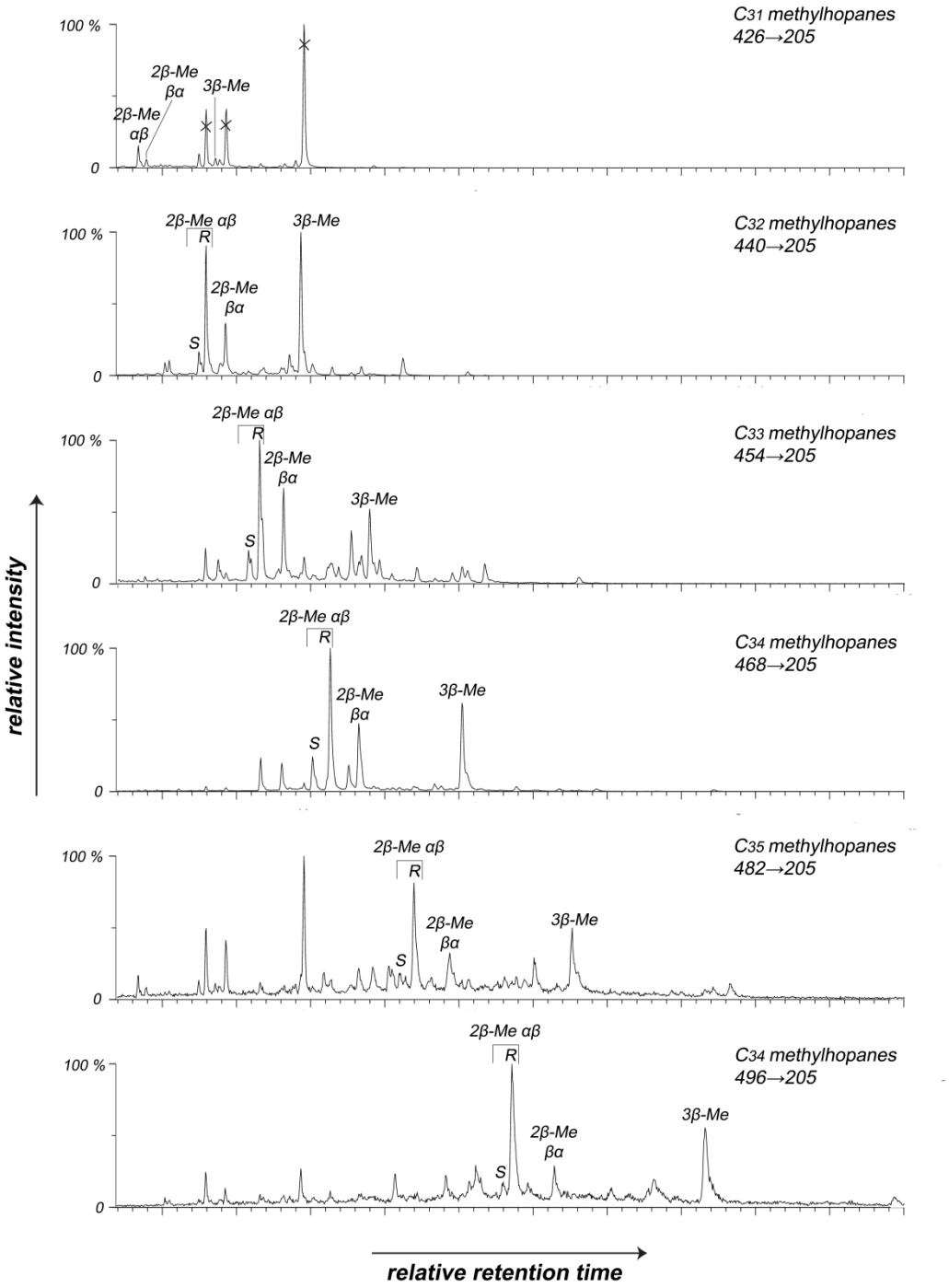

Figure S3: MRM chromatograms showing hopanes in a sample from the analysed core at the depth of 40.3 m. Crossed out peaks mark cross-talk from regular homohopanes. S and R stand for the stereochemistry at C22. Me = methyl.

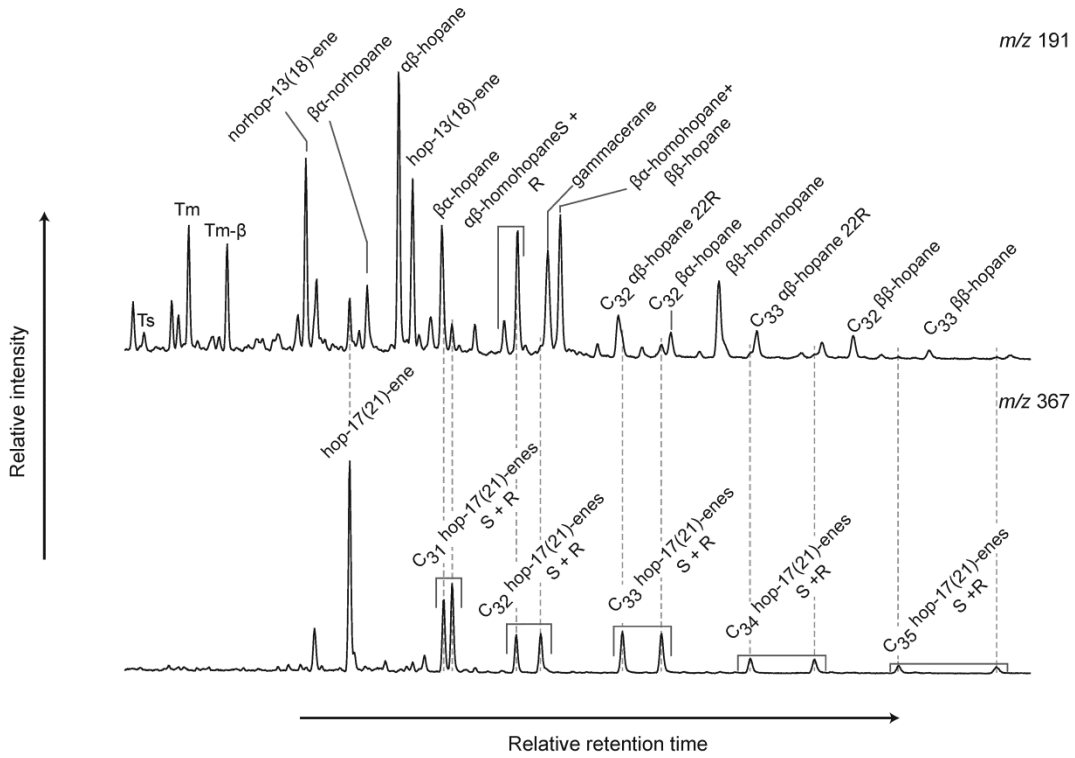

Figure S4: Extracted ion chromatograms of a sample from the analysed core at the depth of 40.3 m showing the distributions of hopanes and hopenes in the aliphatic fraction. S and R stand for the stereochemistry at C22.

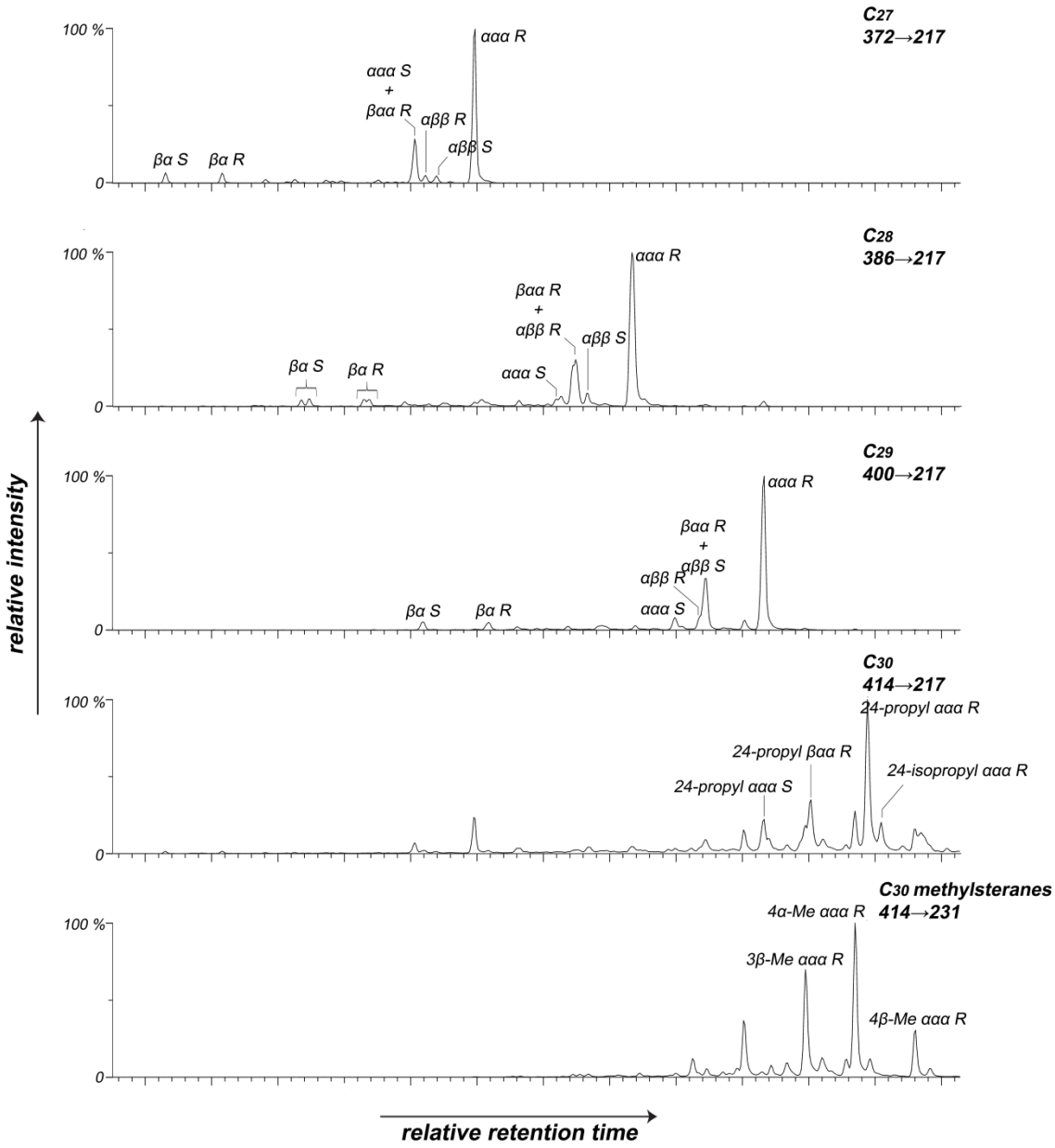

Figure S5: MRM chromatograms showing steranes in a sample from the analysed core at the depth of 40.3 m. S and R stand for the stereochemistry at C20. Me = methyl diasteranes 13β, 17α.

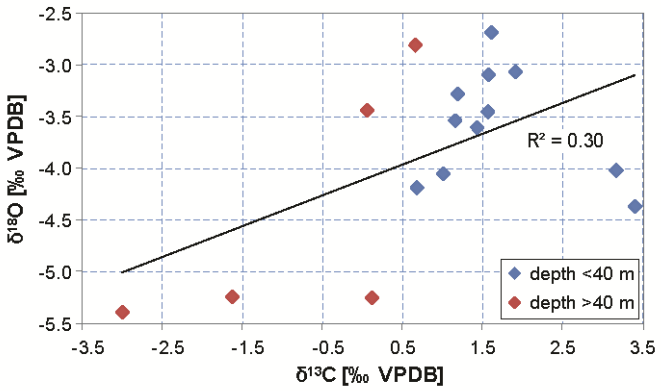

Figure S6: Plot of $\delta^{18}O$ vs $\delta^{13}C$ of carbonates in the MR-1 core.

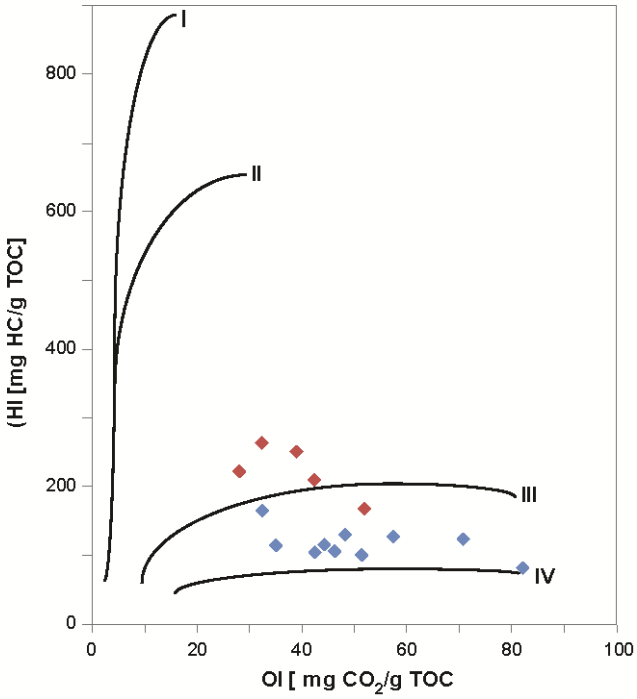

Figure S7: Pseudo van Krevelen diagram of the analysed sediments indicating the kerogen type.

Data included in figures

Table S1: Data included in Fig. 3.

Depth [m]	Pr/Ph	C_{35} HHI [%]	28,30 DNH/ $C_{30}H$	Isor. [µg/g TOC]	Palaeoren. [µg/g TOC]	Monoaryl isopr. [µg/g TOC]			$\delta^{34}S_{pyrite}$ [‰]	Gammacerane index	triMeMTTC/ total MTTCs	$\delta D_{kerogen}$ [‰ VSMOW]	$\delta^{18}O_{carb.}$ [‰ VPDB]
						C_{14}	C_{16}	C_{20}					
27.3	*2.99	1.05	0.01	0.00	*0.00	0.39	0.12	0.03	-24.4	*0.05	*0.79	-109	-4.0
28.1	*2.47	2.04	0.02	0.00	*0.00	0.09	0.03	0.01	n.d	*0.08	*0.83	n.d	-4.2
29.0	*1.47	2.03	0.02	0.00	*0.00	0.53	0.11	0.04	-11.9	*0.11	*0.89	n.d	-3.4
29.7	*1.61	n.d	n.d	0.00	*0.00	0.21	0.08	0.02	-13.6	n.d	*0.88	-115	-3.1
29.9	*1.76	1.70	0.02	0.00	*0.01	0.28	0.09	0.02	n.d	*0.18	*0.88	-121	n.d
30.7	*1.45	1.75	0.04	0.00	*0.00	0.49	0.14	0.04	n.d	*0.05	*0.91	-118	n.d
30.9	*1.31	2.14	0.04	0.00	*0.00	1.27	0.28	0.07	-12.6	*0.16	*0.89	-126	-3.5
31.9	*1.26	2.61	0.04	0.00	*0.03	0.30	0.15	0.04	-16.7	*0.27	*0.91	-113	-3.6
32.8	*1.17	2.66	0.07	0.00	*0.00	0.01	0.08	0.03	-16.5	*0.43	*0.91	-109	-2.7
33.0	*1.29	2.53	0.05	0.00	*0.00	0.01	0.11	0.03	n.d	*0.06	*0.91	-117	n.d
33.2	*0.99	3.36	0.07	0.03	*0.02	0.00	0.03	0.04	-16.5	*0.43	*0.93	-121	-3.1
33.4	*1.00	3.57	0.04	0.00	*0.00	0.00	0.01	0.00	-19.6	*0.24	n.d	n.d	-3.3
34.6	n.d	n.d	n.d	n.d	n.d	n.d	n.d	n.d	-16.0	n.d	n.d	n.d	-4.4
37.8	*0.32	2.67	0.03	0.00	*0.00	0.00	0.00	0.00	-16.2	*0.14	n.d	n.d	-4.0
40.2	*0.39	2.64	0.08	0.00	*0.06	0.02	0.22	0.18	*-24.0	*0.55	*0.95	n.d	-5.2
40.3	*0.41	4.36	0.05	0.58	*2.34	4.18	2.19	1.14	*-13.8	*1.71	*0.95	n.d	-5.4
40.5	*0.51	n.d.	n.d.	0.37	*1.66	2.49	2.11	0.90	n.d	n.d	*0.94	n.d	n.d
40.7	*0.51	3.01	0.04	0.13	*0.50	1.42	1.19	0.49	*-11.9	*1.24	*0.94	-130	-2.8
41.2	*0.48	2.65	0.07	0.25	*1.24	6.62	4.01	1.23	*-15.0	*1.37	*0.95	n.d	-5.2
41.9	*1.00	2.17	0.05	0.02	*0.11	0.19	0.38	0.11	*-19.1	*0.75	*0.93	n.d	-3.4

* published in Tulipani et al. (2014).
n.d. = not determined

Table S2: $\delta^{13}C$ values of the compounds included in Fig. 4 in ‰ *vs.* VPDB. "Ci" stands for monoaryl isoprenoids with the carbon number "i".

Depth [m]	Peak 1 C_{15}	Peak 2 C_{16}	Peak 3 C_{18}	Peak 4 C_{19}	Peak 5 see Fig. 4	Peak 6 See Fig. 4	Peak 7 ?	Peak 8 ?	Peak 9 see Fig. 4	Peak 10 see Fig. 4	Peak 11 palaeorenieratane
40.2	n.d.	n.d.	n.d.	-15.1	-17.8	-20.8	-17.7	-17.0	n.d.	n.d.	n.d.
40.3	n.d.	n.d.	-21.7	-16.8	-18.4	-20.1	-17.0	-16.0	n.d.	n.d.	*-15.3
40.7	-17.2	-16.4	-19.6	-18.6	-16.7	-19.2	-17.9	-17.4	-15.5	-15.9	*-15.4
41.2	n.d.	n.d.	n.d.	n.d.	n.d.	n.d.	n.d.	n.d.	n.d.	n.d.	n.d.
41.9	-19.4	-17.9	-21.2	-19.6	-16.7	-18.9	-17.4	-18.4	n.d.	n.d.	*-15.1

* published in Tulipani et al. (2014).
n.d. = not determined

Table S3: Data included in Fig. 6.

Depth [m]	TOC [wt. %]	TOC_{or} [wt. %]	Carbonates [wt. %]	TN_{org} [wt.%]	TS [wt. %]	C/N [molar]	HI [mg HC/g TOC]	OI [mg CO_2/g TOC]
27.3	0.3	0.7	9.1	0.02	0.3	12.3	70	102
28.1	0.3	1.1	23.7	0.02	0.8	12.3	72	108
29.0	0.5	1.8	15.8	0.02	1.3	19.9	115	35
29.7	0.5	2.1	12.5	0.03	1.6	16.3	124	71
29.9	0.5	2.1	14.7	0.03	1.6	15.8	101	51
30.7	0.6	2.0	11.9	0.03	1.5	15.9	105	42
30.9	0.8	2.8	12.4	0.04	2.0	17.8	166	32
31.9	0.4	1.65	31.8	0.02	1.26	20.4	131	48
32.8	0.5	2.0	12.4	0.03	1.5	15.7	107	46
33.0	0.5	2.3	13.5	0.03	1.8	15.6	128	57
33.2	0.5	2.0	12.8	0.03	1.5	14.9	116	44
33.4	0.1	1.0	65.9	0.00	0.9	28.1	82	82
34.6	0.0	0.2	86.2	0.00	0.2	7.8	38	200
37.8	0.0	0.7	70.3	0.00	0.6	5.9	n.d.	n.d.
40.2	*0.0	0.5	*62.6	0.00	0.5	16.8	n.d.	n.d.
40.3	*0.3	1.0	*68.1	0.01	0.7	17.9	252	39
40.5	*0.9	2.4	*15.2	0.05	1.5	16.8	223	28
40.7	*0.8	2.7	*10.5	0.04	1.9	16.8	211	42
41.2	*0.7	2.1	*32.2	0.04	1.4	18.0	264	32
41.9	*0.7	2.4	*13.3	0.04	1.6	17.6	169	52

* published in in Tulipani et al. (2014).
n.d. = not determined

Table S4: $\delta^{13}C$ values [‰ VPDB] included in Fig. 7 (± standard deviation of at least 2 replicates).

Depth [m]	Carb.	OM	Short-chain *n*-alkanes			Long-chain *n*-alkanes			Phytane	5α 20R steranes		C_{31}-ββ hopane
			C_{16}	C_{19}	C_{21}	C_{25}	C_{27}	C_{29}		C_{27}	C_{29}	
27.3	1.00	-29.74	-31.4 ±0.4	-32.3 ±0.3	-32.4 ±0.4	-32.3 ±0.2	-30.9 ±0.2	-31.7 ±0.4	n.d.	-33.0 ±0.0	n.d.	-30.5 ±0.3
28.1	0.67	-29.88	-32.2 ±0.4	-33.3 ±0.4	-33.0 ±0.4	-32.5 ±0.4	-32.0 ±0.5	-32.0 ±0.4	n.d.	n.d.	n.d.	-31.1 ±0.1
29.0	1.56	-28.25	-28.8 ±0.2	-29.7 ±0.1	-30.1 ±0.1	-28.9 ±0.1	-28.9 ±0.1	-29.1 ±0.1	-31.7 ±0.4	-30.0 ±0.1	-29.0 ±0.2	-28.1 ±0.4
29.7	1.56	-28.19	n.d.	n.d.	n.d.	n.d.	n.d.	n.d.	n.d.	n.d.	n.d.	n.d.
30.9	1.15	-28.40	-29.7 ±0.3	-30.3 ±0.0	-30.6 ±0.2	-29.6 ±0.0	-30.0 ±0.3	-29.4 ±0.1	-31.2 ±0.3	-29.8 ±0.0	-29.8 ±0.3	-28.1 ±0.0
31.9	1.42	-27.83	-29.8 ±0.1	-31.7 ±0.3	-31.3 ±0.4	-30.3 ±0.3	-30.7 ±0.3	-30.0 ±0.3	-31.7 ±0.2	-28.7 ±0.3	-30.3 ±0.4	-28.4 ±0.3
32.8	1.60	-28.56	n.d.	n.d.	n.d.	n.d.	n.d.	n.d.	n.d.	n.d.	n.d.	n.d.
33.2	1.90	-28.30	n.d.	-31.7 ±0.3	-31.9 ±0.2	-30.7 ±0.2	-30.6 ±0.2	n.d.	-32.0 ±0.0	-30.2 ±0.3		-28.9 ±0.1
33.4	1.18	-27.23	-28.3 ±0.4	-29.9 ±0.3	-28.3 ±0.1	-28.0 ±0.1	-27.8 ±0.1	-27.9 ±0.1	-31.4 ±0.0	-29.6 ±0.2	-29.5 ±0.2	-26.6 ±0.4
34.6	3.40	-24.24	n.d.	n.d.	n.d.	n.d.	n.d.	n.d.	n.d.	n.d.	n.d.	n.d.
37.8	3.16	-25.04	n.d.	n.d.	n.d.	n.d.	n.d.	n.d.	n.d.	n.d.	n.d.	n.d.
40.2	0.11	-28.97	-31.1 ±0.3	-32.6 ±0.3	-33.3 ±0.3	-32.4 ±0.1	-32.5 ±0.3	-31.5 ±0.3	-33.5 ±0.0	-32.1 ±0.1	-31.5 ±0.4	-29.3 ±0.0
40.3	-3.01	-29.59	-32.0 ±0.4	-32.5 ±0.20	-32.6 ±0.3	-32.6 ±0.1	-33.1 ±0.4	n.d.	-33.6 ±0.2	-32.8 ±0.4	-31.0 ±0.2	-30.1 ±0.0
40.7	0.65	-28.69	-31.5 ±0.1	-31.8 ±0.4	-32.8 ±0.1	-32.0 ±0.1	-31.8 ±0.3	-30.9 ±0.4	[a]-32.9 ±0.4	-30.9 ±0.0	-30.7 ±0.1	n.d.
41.2	-1.63	-29.01	-31.5 ±0.4	-32.7 ±0.1	-33.1 ±0.1	-32.9 ±0.1	-33.0 ±0.3	n.d.	[a] -32.6 ±0.0	-32.8 ±0.2	-32.0 ±0.3	-30.0 ±0.3
41.9	0.05	-29.21	-31.4 ±0.1	n.d.	n.d.	-33.4 ±0.3	-33.5 ±0.4	-31.7 ±0.2	[b]-33.9 ±0.4	-32.4 ±0.3	-32.5 ±0.2	-30.5 ±0.2

[a] from Tulipani et al (2013).

[b] from Tulipani et al (2014).

n.d. = not determined

Table S5: Data included in Fig. 8.

Depth [m]	Steranes/ hopanes	C_{30} Methylst./C_{27-29} Sts			*iso*-propylchol./ *n*-propylchol.	Pristane/ *n*-C_{17}	Phytane/ *n*-C_{18}	Concentration µg/g TOC						
		3β-Me	4α-Me	4β-Me				Perylene	∑MTTCs	BaPy	BePyr	Bpery	Cor	DBF
27.3	0.20	0.00	0.01	0.00	0.28	0.51	0.16	*0.13	1.83	0.33	0.54	0.96	0.66	0.24
28.1	0.39	0.04	0.02	0.01	0.17	0.77	0.37	*0.02	2.12	0.04	0.06	0.03	0.01	0.01
29.0	0.84	0.07	0.03	0.01	0.11	1.38	0.97	*0.07	7.99	0.12	0.13	0.09	0.05	0.14
29.7	n.d.	n.d.	n.d.	n.d.	n.d.	1.66	1.15	*0.03	3.60	0.03	0.03	0.01	0.00	0.01
29.9	0.76	0.03	0.02	0.01	0.10	1.61	0.95	*0.02	4.04	0.03	0.03	0.02	0.01	0.02
30.7	0.88	0.05	0.03	0.01	0.12	1.86	1.30	*0.05	10.35	0.10	0.11	0.16	0.07	0.17
30.9	1.27	0.06	0.03	0.01	0.13	1.67	1.46	*0.05	12.99	0.07	0.09	0.34	0.14	0.34
31.9	1.44	0.06	0.02	0.01	0.10	2.63	2.15	*0.16	12.20	n.d.	n.d.	n.d.	n.d.	n.d.
32.8	2.47	0.06	0.02	0.01	0.11	2.04	1.61	*0.23	11.56	0.21	0.36	0.60	0.14	0.07
33.0	2.69	0.04	0.02	0.01	0.14	1.82	1.53	*0.23	12.26	0.27	0.36	0.71	0.15	0.08
33.2	3.86	0.05	0.02	0.01	0.12	2.21	2.02	*0.21	10.12	0.23	0.33	0.17	0.04	0.01
33.4	2.37	0.00	0.01	0.00	0.14	0.66	0.94	*0.02	0.45	0.02	0.04	0.02	0.01	0.00
34.6	n.d.	n.d.	n.d.	n.d.	n.d.	n.d.	n.d.	n.d.	n.d.	n.d.	n.d.	n.d.	n.d.	n.d.
37.8	0.49	0.00	0.00	0.00	0.20	0.16	0.66	*0.00	n.d.	0.00	0.01	0.00	0.00	0.00
40.2	4.94	0.08	0.07	0.03	0.13	1.75	4.54	*0.14	6.75	0.03	0.05	0.00	0.00	0.00
40.3	6.36	0.15	0.21	0.07	0.15	3.13	9.35	*1.06	38.54	0.17	0.19	1.08	0.39	0.23
40.5	n.d.	n.d.	n.d.	n.d.	n.d.	4.01	6.99	*0.92	22.42	0.17	0.17	0.90	0.14	0.22
40.7	4.62	0.12	0.34	0.06	0.13	3.09	5.87	*0.54	14.29	0.10	0.11	0.28	0.04	0.09
41.2	2.17	0.10	0.24	0.04	0.20	5.07	11.12	*0.42	21.19	0.07	0.08	0.27	0.03	0.20
41.9	1.17	0.04	0.11	0.02	0.13	3.21	3.67	*0.04	2.68	0.01	0.01	0.01	0.00	0.00

* published in Tulipani et al. (2014).
n.d. = not determined

Table S6: Data included in Fig. 9. Peak areas were inferred from suitable transitions of metastable reaction monitoring-gas chromatography-mass spectrometry (MRM-GC-MS).

Depth [m]	Peak areas		
	∑cholestanes	∑24-methylcholestanes	∑24-ethylcholestanes
27.3	378495	124937	678755
28.1	1993635	707340	3861990
29.0	10189203	3458112	17904085
29.7	n.d.	n.d.	n.d.
29.9	5618845	2099182	10484379
30.7	8955227	3410066	17844243
30.9	20036199	7667875	35901309
31.9	9733470	3956699	20775005
32.8	11028498	4975431	22450442
33.0	24274101	11377345	48922215
33.2	30561811	14750194	64474802
33.4	1022704	417535	2507036
34.6	n.d.	n.d.	n.d.
37.8	326084	102564	511516
40.2	5677128	2771224	9992119
40.3	51521847	25616683	82671752
40.5	n.d.	n.d.	n.d.
40.7	15859006	7138781	19431634
41.2	10344653	4529279	13476443
41.9	2382601	1215802	4162140

n.d. = not determined

References in SM

Fossing, H., and Jørgensen, B., 1989, Measurement of bacterial sulfate reduction in sediments: Evaluation of a single-step chromium reduction method: Biogeochemistry, v. 8, no. 3, p. 205-222.

Mann, J.L., Vocke, R.D., Kelly, W.R., 2009. Revised $\delta^{34}S$ reference values for IAEA sulfur isotope reference materials S-2 and S-3. Rapid Communications in Mass Spectrometry 23, 1116-1124.

Paul, D., Skrzypek, G., 2007. Assessment of carbonate-phosphoric acid analytical technique performed using GasBench II in continuous flow isotope ratio mass spectrometry. International Journal of Mass Spectrometry 262, 180-186.

Schimmelmann, A., Lewan, M.D., Wintsch, R.P., 1999. D/H isotope ratios of kerogen, bitumen, oil, and water in hydrous pyrolysis of source rocks containing kerogen types I, II, IIS, and III. Geochimica et Cosmochimica Acta 63, 3751-3766.

Schimmelmann, A., Sessions, A.L., Mastalerz, M., 2006. Hydrogen isotopic (D/H) composition of organic matter during diagenesis and thermal maturation. Annual Review of Earth and Planetary Sciences 34, 501-533.

Sauer, P.E., Schimmelmann, A., Sessions, A.L., Topalov, K., 2009. Simplified batch equilibration for D/H determination of non-exchangeable hydrogen in solid organic material. Rapid Communications in Mass Spectrometry 23, 949-956.

Skrzypek, G., Paul, D., 2006. δ13C analyses of calcium carbonate: comparison between the GasBench and elemental analyzer techniques. Rapid Communications in Mass Spectrometry 20, 2915-2920.

Tulipani, S., Grice, K., Greenwood, P. & Schwark, L., 2013. A pyrolysis and stable isotopic approach to investigate the origin of methyltrimethyltridecylchromans (MTTCs). Organic Geochemistry 61, 1-5

Tulipani, S., Grice, K., Greenwood, P., Schwark, L., Böttcher, M.E., Summons, R.E., Foster, C.B., 2014. Molecular Proxies as Indicators of Freshwater Incursion-Driven Salinity Stratification. Global Biogeochemical Cycles (in review)

Wood, G., Gabriel, A., Lawson, J., 1996. Palynological techniques-processing and microscopy. American Association of Stratigraphic Palynologists Foundation.